

Differential gene co-expression networks via Bayesian biclustering models

Chuan Gao

*Department of Statistical Science
Duke University
Durham, NC 27705, USA*

CHUAN.GAO@DUKE.EDU

Shiwen Zhao

*Computational Biology and Bioinformatics
Duke University
Durham, NC 27705, USA*

SHIWEN.ZHAO@DUKE.EDU

Ian C McDowell

*Computational Biology and Bioinformatics
Duke University
Durham, NC 27705, USA*

IAN.MCDOWELL@DUKE.EDU

Christopher D Brown

*Department of Genetics
University of Pennsylvania
Philadelphia, PA 19104, USA*

CHRBRO@MAIL.MED.UPENN.EDU

Barbara E Engelhardt

*Department of Computer Science
Princeton University
Princeton, NJ 08540, USA*

BEE@PRINCETON.EDU

Abstract

Identifying latent structure in large data matrices is essential for exploring biological processes. Here, we consider recovering gene co-expression networks from gene expression data, where each network encodes relationships between genes that are locally co-regulated by shared biological mechanisms. To do this, we develop a Bayesian statistical model for *biclustering* to infer subsets of co-regulated genes whose covariation may be observed in only a subset of the samples. Our biclustering method, *BicMix*, has desirable properties, including allowing overcomplete representations of the data, computational tractability, and jointly modeling unknown confounders and biological signals. Compared with related biclustering methods, BicMix recovers latent structure with higher precision across diverse simulation scenarios. Further, we develop a method to recover gene co-expression networks from the estimated sparse biclustering matrices. We apply BicMix to breast cancer gene expression data and recover a gene co-expression network that is differential across ER+ and ER- samples.

1. Introduction

Cellular mechanisms by necessity tightly regulate the spatiotemporal transcription of all genes. Gene transcription is not independently regulated across genes: many of the mechanisms regulating transcription affect multiple genes simultaneously. Functional *gene mod-*

ules consist of subsets of genes that share similar expression patterns and perform coordinated cellular functions (Hung *et al.*, 2010; Parkkinen and Kaski, 2010). If we consider each gene as a vertex in a network, then pairs of genes within a gene module for which the correlation in expression levels cannot be explained by other genes will be connected by an undirected edge. Across all functional gene modules, these pairwise relationships constitute gene co-expression networks. Constructing these undirected gene networks, as compared to clustering genes into gene modules (Eisen *et al.*, 1998; Jiang *et al.*, 2004; Reich *et al.*, 2006; Souto *et al.*, 2008), provides rich detail about pairwise gene relationships. An even richer structure capturing these pairwise relationships would be a directed network of genes, but currently directed networks are computationally intractable to construct relative to undirected gene networks (Friedman *et al.*, 2000; Davidich and Bornholdt, 2008; MacNeil and Walhout, 2011; Karlebach and Shamir, 2008). This work describes an approach to compute an undirected gene co-expression network from a probabilistic model that clusters both genes and samples.

Several algorithmic methods have been proposed to construct gene co-expression networks by partitioning a set of genes (and, in some cases, samples) into gene modules from which an undirected graph is elicited (Zhang and Horvath, 2005; Ruan *et al.*, 2010). In most cases, gene partitioning creates disjoint sets of genes, implying that genes only participate in a single gene module; biologically this assumption does not hold, and the impact is that the gene networks based on disjoint models are not well connected. These approaches are not probabilistic, and thus uncertainty in the clustering is not well characterized. In our work, we take a flexible statistical approach to modeling relationships in gene expression data.

1.1 Latent factor models for gene expression data.

Latent factor models are often used to identify groups of co-regulated genes in gene expression data (Engelhardt and Stephens, 2010; Carvalho *et al.*, 2008; West, 2003; Bhattacharya and Dunson, 2011). In particular, latent factor models decompose a matrix $\mathbf{Y} \in \mathbb{R}^{p \times n}$ of p genes and n samples into the product of two matrices, $\mathbf{\Lambda} \in \mathbb{R}^{p \times K}$, the factor loadings, and $\mathbf{X} \in \mathbb{R}^{K \times n}$, the latent factor matrix, for K latent factors, and assuming independent Gaussian noise. Because it is costly to obtain and assay genome-wide gene expression levels in a single sample, most gene expression studies include observations of many more genes p than samples n . This so-called $p \gg n$ scenario limits our ability to find latent structure in this expansive but underconstrained space and suggests the use of strong regularization on the factors and loadings to provide structure for this optimization problem. For example, we may regularize a latent space to exclude a feature from contributing to all but a few latent factors through the application of encouraging sparse loading vectors (Witten *et al.*, 2009; Engelhardt and Stephens, 2010). The resulting sparse loading matrix enables non-disjoint gene clusters to be extracted from a fitted latent factor model (Carvalho *et al.*, 2008). Sparse latent factor models are much more interpretable than their non-sparse counterparts, but are generally limited to finding a small number K of large clusters for reasons that include computational tractability and robustness.

Given the complexity of biological systems, manifested as tens of thousands of genes, subsets of which are transcriptionally regulated by possibly a larger number of mechanisms,

a more appropriate model might create a large number K of gene clusters that each contain small numbers of genes. Constructing an *overcomplete* representation of the data, where the number of latent factors is larger than the number of samples, has proven effective for a variety of applications in classical statistics (Aharon et al., 2006; Mairal et al., 2010; Witten et al., 2009; Zhou et al., 2009; Xing et al., 2012). However, building such a method is difficult because, without careful regularization, the recovered factors are not robust or interpretable, and signals that account for a small proportion of the variation in the gene expression data are not reproducibly recovered.

Besides encouraging sparsity in the factor loading matrix, which results in non-disjoint clusters of genes that co-vary across all samples, one can also induce sparsity in the factor matrix, which results in non-disjoint subsets of samples within which small number of genes uniquely exhibit co-variation. Mathematically, this corresponds to regularizing both factor and loading matrices using priors that induce zero-valued elements. Biologically, biclustering model components identify covariation among a small number of genes that is exclusive to, for example, samples from adipose tissue. This approach addresses a general problem known as biclustering (Cheng and Church, 2000; Ben-Dor et al., 2003; Murali and Kasif, 2003; Li et al., 2009; Preli et al., 2006; Bergmann et al., 2003; Huttenhower et al., 2009; Lazzeroni and Owen, 2000; Gu and Liu, 2008; Bozda? et al., 2009; Hochreiter et al., 2010; Kluger et al., 2003; Aguilar-Ruiz, 2005). A biclustering model decomposes a data matrix into clusters that each correspond to a subset of samples and a subset of features that exhibit latent structure. Our flexible Bayesian approach allows each sample and each gene to belong to any number of the K latent clusters or *components* (i.e., a sparse loading vector of length p and a sparse factor vector of length n), and does not require orthogonality across the factors or loadings.

1.2 Capturing independent sources of variation in gene expression data.

Gene expression levels have been shown to be sensitive to a number of environmental and technical covariates such as batch, sex, ethnicity, smoking status, or sample tissue heterogeneity. Methods to adjust the observation matrix to remove the effects of these covariates without eliminating signals of interest have been proposed, but most attempts have been limited to correcting for confounding effects in a preprocessing step (Pickrell et al., 2010; Brown et al., 2013) or correcting for confounding effects jointly with univariate association testing (Leek and Storey, 2007; Stegle et al., 2010; Listgarten et al., 2010). The two-stage approach applied to estimates of co-expression network have not been successful: often variation in expression levels of large gene modules are captured in the confounding effects and controlled in the first step. Because of the exploratory nature of this method, we will not include association testing in our models, but instead develop factor analysis-based methods to recover all of the sources of co-variation in the observed data matrix in an unsupervised way (Gao et al., 2013). To recover gene co-expression signals in the presence of large-scale co-variation due to confounders, we have found that two properties of the statistical model are essential: i) co-regulated genes and confounding effects need to be modeled jointly, and ii) the number of gene clusters and the number of confounding effects must be estimated from, and scale with, the observed data (Gao et al., 2013).

In this paper, we develop Bayesian statistical model for biclustering called *BicMix*. Our motivation behind developing this method was to identify large numbers of subsets of co-regulated genes capturing as many unique sources of gene transcription variation as possible. We next developed a simple method to reconstruct gene co-expression networks based on the sparse covariance matrices reconstructed using our biclustering model. This method recovers different types of gene co-expression networks, categorized by quantifying the contribution of each sample to the gene cluster: i) ubiquitously-expressed co-expression networks, ii) co-expression networks specific to a sample subtype, and iii) networks that are differentially co-expressed across sample subtypes. We apply this approach to two gene expression data sets without correcting for confounding effects in the gene expression levels. We apply our biclustering model to gene expression levels measured in heterogeneous breast cancer tissue samples (Vant Veer *et al.*, 2002; Van de Vijver *et al.*, 2002) to recover a co-expression network that is differentially expressed across ER+ and ER- samples.

2. Results

2.1 Bayesian Biclustering using BicMix.

Biclustering was first introduced to detect clusters of states and years that showed similar voting patterns among Republicans in national elections (Hartigan, 1972) and was later referred to as *biclustering* to identify similarly expressed genes (Cheng and Church, 2000). It has also been referred to as two mode clustering (Van Mechelen *et al.*, 2004), subspace clustering (Patrikainen and Meila, 2006; Kriegel *et al.*, 2009), or co-clustering (Yoon *et al.*, 2007) in various applied contexts. Biclustering was used successfully to explore latent sparse structure in different applied domains (Busygin *et al.*, 2008), including gene expression data (Cheng and Church, 2000; Madeira and Oliveira, 2004, 2009; Ben-Dor *et al.*, 2003; Turner *et al.*, 2005; Santamara *et al.*, 2007), neuroscience (Neng Fan, 2009), time series data (Madeira and Oliveira, 2009), and collaborative filtering (de Castro *et al.*, 2007). There are a few comprehensive reviews of biclustering for further details (Preli *et al.*, 2006; Eren *et al.*, 2012).

Biclustering approaches fall into four general categories. The first category of biclustering assumes that each gene is a linear combination of a mean effect, a column effect, and a row effect, some of which may be zero (Cheng and Church, 2000). One approach in this category, *plaid*, assumes that the gene effects are the sum of many sparse submatrix components, where each submatrix includes non-zero values only for a small number of genes and a small number of samples (Lazzeroni and Owen, 2000; Gu and Liu, 2008). The second category of biclustering method explicitly identifies similar samples and features in the data matrix and groups them together through hierarchical clustering (Eisen *et al.*, 1998). For example, samples may be clustered by considering some measure of feature similarity (Ben-Dor *et al.*, 2003; Bergmann *et al.*, 2003; Murali and Kasif, 2003; Aguilar-Ruiz, 2005; Bozda? *et al.*, 2009). The third category of biclustering method builds up biclusters by iteratively grouping features in a greedy way (e.g., identifying all genes that have correlated expression levels with a selected gene) and then removing samples that do not support that grouping (Li *et al.*, 2009). The last category of biclustering method uses Bayesian sparse factor analysis models (Hochreiter *et al.*, 2010). These models decompose a gene expression matrix into two sparse matrices. Sparsity-inducing priors, such as the Laplace prior, are imposed

on both the loading and the factor matrices to produce zero-valued elements in the two latent matrices. Our approach falls into this last category of a sparse statistical model for biclustering.

Specifically, we developed a Bayesian biclustering model, *BicMix*, built on factor analysis with sparsity-inducing priors on both of the low dimensional matrices. In particular, we define the following latent factor model for matrix $\mathbf{Y} \in \mathbb{R}^{p \times n}$, which is the set of observations for p genes across n samples:

$$\mathbf{Y} = \mathbf{\Lambda}\mathbf{X} + \epsilon \tag{1}$$

where $\mathbf{\Lambda} \in \mathbb{R}^{p \times K}$ is the *loading matrix*, $\mathbf{X} \in \mathbb{R}^{K \times n}$ is the *factor matrix*, $\epsilon \in \mathbb{R}^{p \times n}$ is the residual error matrix, and K is fixed a priori. We assume that the residual error is independent across genes and samples and has a zero-mean multivariate Gaussian distribution with gene-specific variance: $\epsilon_{.,i} \sim \mathcal{N}_p(0, \mathbf{\Psi})$ for $i = 1, \dots, n$, where $\mathbf{\Psi} = \text{diag}(\psi_1, \dots, \psi_p)$. While a value must be given for K , the number of latent factors, the model removes factors when appropriate, so K should be an overestimate of the number of latent factors.

To induce sparsity in both the factors and the loadings, we used the three parameter beta (\mathcal{TPB}) distribution (Armagan et al., 2011), which has been shown to be computationally efficient and to induce flexible modeling behavior as a sparsity-inducing prior. In previous work (Gao and Engelhardt, 2012; Gao et al., 2013), we included three layers of regularization via the \mathcal{TPB} distribution to induce sparsity in the loadings matrix; we extended this model to include this same sparsity-inducing prior on the factor matrix (see Appendix A). With this prior on both the factor and loadings matrices, the model becomes a biclustering model, estimating subsets of genes for which correlation is only observed in a subset of samples. This structured prior produces favorable properties in this biclustering model: i) the number of factors and loadings are determined by the data, because the sparsity-inducing prior removes unnecessary factors; ii) each factor and corresponding loading has a different level of shrinkage applied to it, enabling a non-uniform level of sparsity and corresponding percentage of variance explained (PVE) for each factor and loading pair (Gao et al., 2013); iii) neither the clusters of genes nor the clusters of samples are disjoint, so all genes and all samples may be in any number of clusters, or none; and iv) strong regularization allows overcomplete estimates of the response matrix, with possibly more factors K than samples n .

In gene expression data, observed covariates or unobserved confounding effects may systematically influence variation in the observation (Leek and Storey, 2007; Listgarten et al., 2010; Stegle et al., 2010). As in prior work, we tailored our sparsity-inducing prior to jointly model these often dense confounding effects (Gao et al., 2013). In particular, we adapted our model so that the loadings and factors are drawn from a two-component mixture distribution, where each vector is either sparse—with many zeros—or dense—with no zeros (Figure 1). We extract information about whether a vector is sparse or dense directly from the fitted model parameters using the expected value of the mixture component assignment variables for each component $k = 1, \dots, K$, where $z_k \in \{0, 1\}$ indicates a dense or a sparse loading and $o_k \in \{0, 1\}$ indicates a dense or a sparse factor. This two-component mixture in the prior distribution for the factors and loadings adds two additional favorable properties to the biclustering model. First, it jointly models covariates that regulate variation in most genes and also in few genes; we have found that confounding effects are often captured

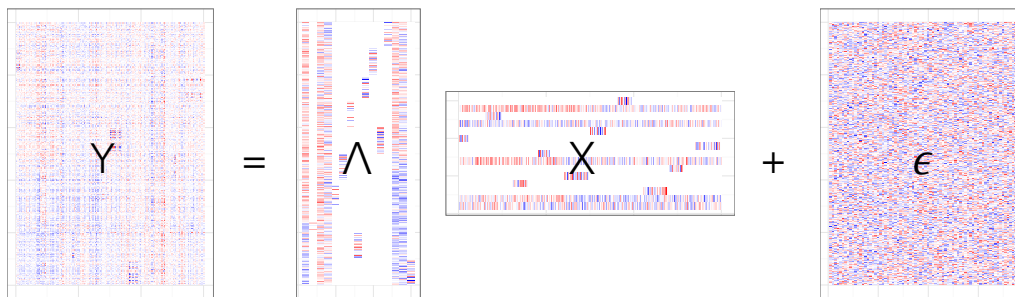


Figure 1: **Schematic representation of the BicMix biclustering model.** Ordered from left to right are, respectively, the $p \times n$ gene expression matrix \mathbf{Y} , the $p \times K$ loading matrix $\mathbf{\Lambda}$ including both sparse and dense columns, the $K \times n$ factor matrix \mathbf{X} including both sparse and dense rows, and the $p \times n$ residual error ϵ . Blue, red and white entries in each matrix correspond to negative, positive, and zero values, respectively. In the response matrix \mathbf{Y} , the p genes are on the rows and n samples are on the columns.

in the dense components as large numbers of samples and genes are affected (e.g., batch effects) (Leek *et al.*, 2010; Gao *et al.*, 2013). Second, it has the effect of relaxing a computationally intractable space, enabling robust and scalable parameter estimation in a Bayesian framework. Specifically, considering all possible subsets of genes and samples to identify biclusters is intractably difficult; however, it is computationally tractable to first search over the space for which cluster membership is a continuous value and then subsequently identify clusters by iteratively shrinking to zero elements with membership values near zero. We estimate parameters in this model using both Markov chain Monte Carlo (MCMC) approaches and a variational Expectation-Maximization (EM) approach; see Appendix A and B for details.

2.2 Simulations and comparisons.

We simulated data from an alternative generative model for the observations matrix $\mathbf{Y} = \mathbf{\Lambda}\mathbf{X} + \epsilon$, where \mathbf{Y} has dimension $p = 500$ by $n = 300$ and $\epsilon_{i,j} \sim \mathcal{N}(0, \nu)$. Within this model, we simulated sparsity as follows: for each loading and factor, a number $m \in [5, 20]$ of elements were randomly selected and assigned values drawn from $\mathcal{N}(0, 2)$; the remaining elements were set to zero. We allowed components to share as many as five elements. Simulation 1 (Sim1) has ten sparse components. Simulation 2 (Sim2) has ten sparse components and five dense components, for which the loadings and factors were drawn from a $\mathcal{N}(0, 2)$ distribution. The components were shuffled so that a sparse loading may correspond to a dense factor, and vice versa. For both simulations we considered low and high noise scenarios, so the residual error simulation parameter in the low noise (LN) setting was $\nu = 1$ and the high noise (HN) setting was $\nu = 2$. Each simulation was repeated ten times.

We ran BicMix and five other biclustering methods—Fabia (Hochreiter *et al.*, 2010), Plaid (Lazzeroni and Owen, 2000), CC (Cheng and Church, 2000), Bimax (Preli *et al.*, 2006), and Spectral biclustering (Kluger *et al.*, 2003)—on the simulated data. For all

simulations, we ran BicMix by setting $a = b = c = d = e = f = 0.5$ and $\nu = \xi = 1$ to recapitulate the horseshoe prior at all levels of the hierarchy. The algorithm was initialized with warm start values by running MCMC for 100 iterations and using the final sample as the initial state for variational EM. For BicMix results, components that are classified as sparse are not thresholded post hoc, because our parameter estimation tends to compute zero for these values. All other methods were run using their recommended settings (details in Appendix C). For Sim2, we corrected the simulated data for the dense components by controlling for five PCs before all other methods were run; without this initial correction for dense components, results from the other biclustering methods were uninterpretable. For all runs, BicMix was initialized with $K = 50$ latent factors; all other methods were initialized with the correct number of sparse factors $K = 10$. For Fabia, we ran the software in two different ways. The results from running Fabia with the recommended settings are denoted as *Fabia*. We also set the sparsity threshold in Fabia to the number (from 100 quantiles of the uniform distribution over $[0.1, 5]$) that produced the closest match in the recovered matrices to the number of non-zero elements in the simulated data; we label these results *Fabia-truth*.

We used the *recovery and relevance score* (R&R score) (Preli et al., 2006) to measure the power and accuracy of each method in recovering true biclusterings. Let the true set of sparse matrices be \mathbf{M}_1 and the recovered set of sparse matrices be \mathbf{M}_2 ; then the R&R score is calculated as:

$$\text{Rec} = \frac{1}{|\mathbf{M}_1|} \sum_{b_1 \in \mathbf{M}_1} \max_{b_2 \in \mathbf{M}_2} \frac{b_1 \cap b_2}{b_1 \cup b_2}, \quad (2)$$

$$\text{Rel} = \frac{1}{|\mathbf{M}_2|} \sum_{b_2 \in \mathbf{M}_2} \max_{b_1 \in \mathbf{M}_1} \frac{b_1 \cap b_2}{b_1 \cup b_2}. \quad (3)$$

Recovery quantifies the proportion of true clusters that are recovered (i.e., recall); *relevance* refers to the proportion of true clusters identified in the recovered clusters (i.e., precision). For BicMix, we applied this R&R score to the components for which both the loading and the factor were sparse, which indicates a biclustering. For the doubly-sparse latent factor models, Fabia, and BicMix, we also calculated a sparse stability index (SSI) (Gao et al., 2013) to compare the recovered and true matrices; SSI is invariant to label switching and scale.

For Sim 1, we found that BicMix recovered the sparse loadings, sparse factors, and the biclustering well in the low noise scenario based on both RR (Figure 2a) and SSI (Figure 2b). Fabia had the second best performance based on RR and SSI. For comparison, Fabia-truth achieved better R&R scores than Fabia (Figure 2a); the clustering results from BicMix dominated those from Fabia-truth, although there was only a small gain in relevance in the low noise Sim1 results for BicMix. Plaid showed high relevance for the recovered biclusters regardless of the noise level for Sim1, but at the expense of poor recovery scores. The remaining methods did not perform well in these simulations with respect to the R&R score.

For Sim2, BicMix correctly identified the sparse and dense components (Figure 2a), where a threshold of $\langle z_k \rangle > 0.9$ was used to determine when a loading k was dense. The performance of Fabia on Sim2 deteriorated substantially relative to its performance on

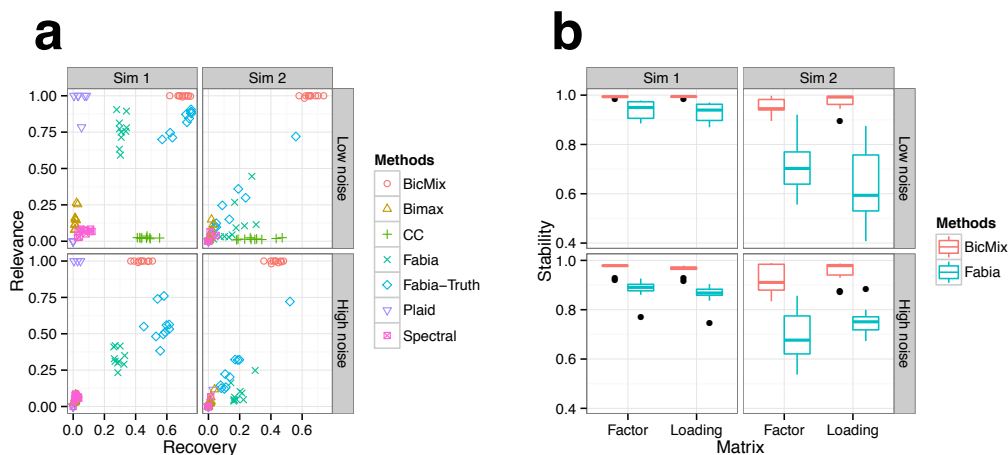


Figure 2: **Comparison of BicMix with related methods.** Top row: simulation with low noise, bottom row: simulation with high noise. Left column: Sim1 with only sparse components, right column: Sim2 with sparse and dense components. Panel a: Recovery score on the x-axis, relevance score on the y-axis for all methods in the legend. Panel b: Stability statistic (y-axis) for the sparse components recovered by BicMix and Fabia.

Sim1, although the confounders were removed from the data using the correct number of PCs and the correct number of factors was given. For both BicMix and Fabia, additional noise in the simulation made bicluster recovery more difficult, as shown in deterioration of the recovery score for both methods; however, unlike Fabia, the relevance score of the biclustering from BicMix was unaffected by additional noise in Sim2-HN. The other methods show inferior performance relative to BicMix and Fabia on this simulation. CC assumes that genes in each bicluster have constant expression values, which limits its ability to cluster genes with heterogeneous expression levels. Bimax assumes binary gene expression values (i.e., over- or under-expressed), which also limit its utility for heterogeneous expression levels. Spectral biclustering methods impose orthogonal constraints on the biclusters; this orthogonality assumption is certainly violated in the simulations we designed here and also in gene expression data.

GENE CO-EXPRESSION NETWORKS FROM BICLUSTERS.

To construct an undirected gene network, we built a Gaussian Markov random field, or a Gaussian graphical model (GGM) (Schafer and Strimmer, 2005a), using the components recovered from our biclustering model (Appendix D). In particular, regularized estimates of the gene-by-gene covariance matrix may be computed from our parameter estimates; factor analysis is often viewed as a method for low-rank covariance estimation by marginalizing over the factors, \mathbf{X} . Furthermore, for any subset of components with sparse loading vectors, $A \subseteq \{1, \dots, K\}$, $\Omega_A = \Lambda_A \Sigma_{A,A} \Lambda_A^T + \Psi$, where $\Sigma_{A,A}$ is the covariance matrix for \mathbf{X}_A , estimates a regularized covariance matrix for the genes loaded on Λ_A . Note that Ω_A is both sparse and full rank; biclustering is a highly structured approach to estimating

regularized covariance matrices (Schafer and Strimmer, 2005b). The inverted covariance matrix is a symmetric precision matrix $\Delta_{\mathbf{A}} = \Omega_{\mathbf{A}}^{-1}$, where $\Delta_{i,j}$ quantifies the pairwise partial correlation between genes i and j . The intuition is that, in a GGM, edges are defined as pairs of nodes for which the partial correlation is non-zero. Since each loading Λ_i , $i \in A$, specifies a cluster of genes, we do not invert the full covariance matrix, but instead invert the submatrix that corresponds to genes with non-zero loadings in those components. This approach avoids inducing edges between genes that never occur in the same cluster. We used GeneNet (Schafer and Strimmer, 2005a) to test the precision matrix for significant edges. GeneNet assumes that the edges are drawn from a mixture of the null (no edge) and alternative (edge) distributions, $f(E) = \eta_0 f_0(E) + \eta_A f_A(E)$ to calculate the probability of each edge being present or not. Practically, we selected edges with a probability of > 0.8 .

To recover co-variance networks with particular semantics with respect to the samples, we choose the subset of components that contribute to this covariance matrix carefully. In particular, when we select subset A to include only components that have non-zero factors in a single tissue, we identify tissue-specific components. When we select A such that all samples have a non-zero contribution to a component, we recover ubiquitous components. And when we select A such that the mean ranks of the values for one covariate type is different than the mean ranks of values for a different covariate type, we identify components that are differential across the two covariate types.

2.3 Breast cancer network

We investigated a breast cancer data set that contains 24,158 genes assayed in 337 breast tumor samples (van 't Veer et al., 2002; Van de Vijver et al., 2002; Schroeder et al., 2011) after filtering for genes that are $> 10\%$ missing and imputing the rest of the missing values (Hastie et al., 1999) (Appendix C). All patients in this data set had stage I or II breast cancer and were younger than 62 years old. Among the 337 patients, 193 had lymph-node negative disease and 144 had lymph-node positive disease; prognostic signatures such as *BRCA1* mutations, Estrogen Receptor (ER), Distant Metastasis Free Survival (DMFS) were also collected for all patients. We focused on building differential gene co-expression networks across ER positive (ER+) and ER negative (ER-) patients because of ER's prognostic value in profiling breast cancer patients (Zhang et al., 2014): cancer patients that are ER+ are more likely to respond to endocrine therapies than patients that are ER-. In these data, there are 249 ER+ and 88 ER- patients as compared to 97 *BRCA1* mutation carriers, two *BRCA2* mutation carriers and 97 patients with no *BRCA* mutations.

We ran *BicMix* on these data, setting $a = b = c = d = e = f = 0.5$ and $\nu = \xi = 1$ to recapitulate the horseshoe prior, as in the simulations; the initial number of components was set to $K = 300$. *BicMix* was run for 5,000 iterations starting from 177 random values. We first removed factors that were zero; then we removed components for which the number of genes in the loading and the number of samples in each factor had changed in the most recent 2,000 iterations of EM, indicating lack of stability. We recovered 4,721 components across 177 runs, of which 9 loadings and 1,632 factors were dense (Figure 3a,b).

The distribution of the number of genes in each sparse component was skewed to small numbers (Figure 3a). We categorized each component as one of four types of configurations: sparse gene loadings with sparse sample factors (SS), sparse gene loadings with dense sample

factors (SD), dense loadings with sparse factors (DS), and dense loadings with dense factors (DD). SS components will capture subsets of genes that are uniquely co-expressed in a subset of samples (e.g., ER+ specific interactions). SD components capture subsets of genes that are differentially co-expressed among all samples (e.g., sex-differential networks, batch effects). DS components capture a subset of samples in which all genes have additional co-variation (e.g., sample contamination). DD components capture variation that occurs across all samples and affects co-variation across all genes (e.g., latent population structure).

For each random run, we calculated the percentage of variance explained (PVE) per component as $\frac{Tr(\Lambda_i(X_i X_i^T)\Lambda_i^T)}{Tr(\Lambda(\mathbf{X}\mathbf{X}^T)\Lambda^T)}$, where Tr denotes the trace operator. We ordered the components by PVE within each SS, SD, DS, and DD component category. We calculated the mean, maximum, and minimum values of the PVE-ordered, categorized components across the random runs. Note that, because there are no orthogonality constraints, it is possible that many of these components explain similar variation in the observations; for this quantification we are assuming this PVE is disjoint and normalizing across all component-wise PVEs. We also calculated the total PVE explained by each component category by summing the total PVE for all components jointly in each category. The distribution of the number of genes contained in each loading and the PVE by component and across SD, SS, DS, DD categories show (Figure 5). The number of components that fell into the SS, SD, DS, DD categories accounted for 65.3%, 34.5%, 0.085%, 0.1%, respectively, of the total number of components. In the same order, components in the four categories accounted for 23.3%, 76%, 0.5% and 0.2% of the total PVE.

We selected components from the fitted BicMix model to identify ER+ and ER- specific gene clusters (Appendix D). Moreover, to select gene clusters that were differentially expressed across ER+ and ER- samples, we identified components corresponding to factors that had a significant difference in the mean rank of the factor value between the ER+ and ER- samples based on a Wilcoxon rank sum test (threshold $p \leq 1 \times 10^{-10}$). Across our components, we found 41 components unique to ER+ samples, 183 components unique to ER- samples, and 812 components that were differential across ER+ and ER- samples (Figure 3c,d).

The precision matrices of the subsets of components corresponding to the three network subtypes were constructed and edges among these genes were tested using our method for extracting gene co-expression networks from the fitted biclustering model (Appendix D) (Schafer and Strimmer, 2005a). For the ER- specific network, we recovered a total of 216 genes and 728 edges; for the ER+ specific network, we recovered 932 genes and 5,383 edges (Supplemental Figures S2-S3; Supplemental Tables S13-14). There were no replicated edges for the ER+ samples and ten edges that were replicated two or more times. We confirmed that there were no nodes and edges shared across the two specific networks. There were ten genes that were shared across the two specific networks.

For the network of differential co-expression across ER+ and ER- samples, we recovered 90 genes and 357 edges that were replicated > 10 times across the 177 runs (Figure 4), Supplemental Table S15). We hypothesised that, because the network was differential, the 90 genes may be divided into two sub-groups: a group of genes that are up-regulated in the ER+ samples and down-regulated in the ER- samples, and a group of genes that are down-regulated in the ER+ samples and up-regulated in the ER- samples. To test this

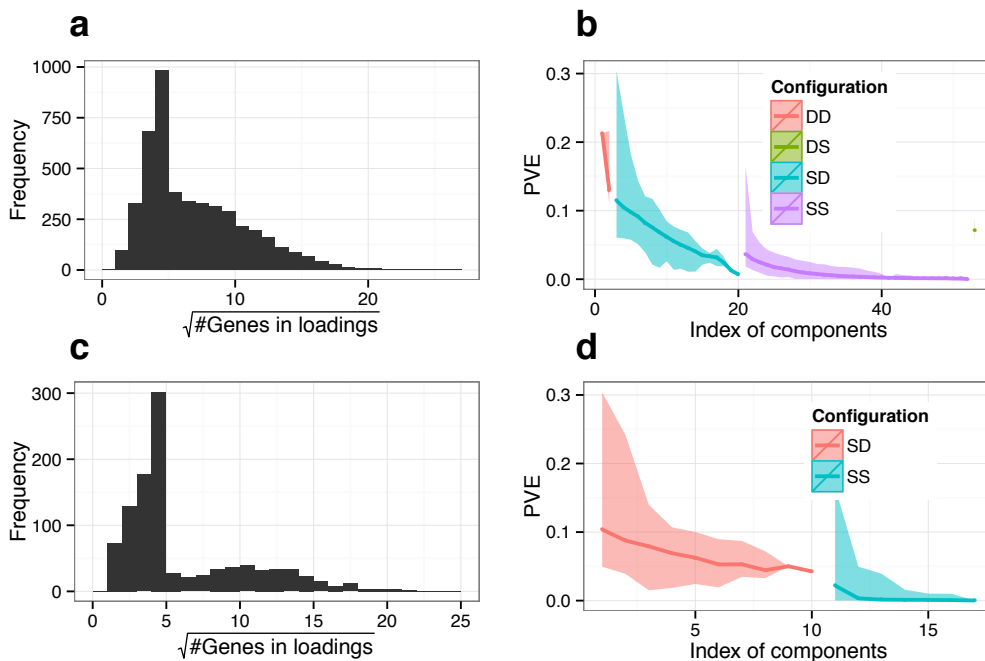


Figure 3: **Distribution of the number of genes and PVE in the breast cancer data.** Panel a: Distribution of the number of genes for the 4,751 components. Panel b: PVE for two DD components, 50 SD components, 50 SS components and one DS component. Panel c: Distribution of the number of genes for the 1,036 components that are ER- specific, ER+ specific, and ER differential. Panel d: PVE for all components that are ER-, ER+, and ER differential (SS and SD only). For panels b and d, the middle lines show the median PVE, the ribbons show the range of the minimum and maximum value of PVE across 177 runs.

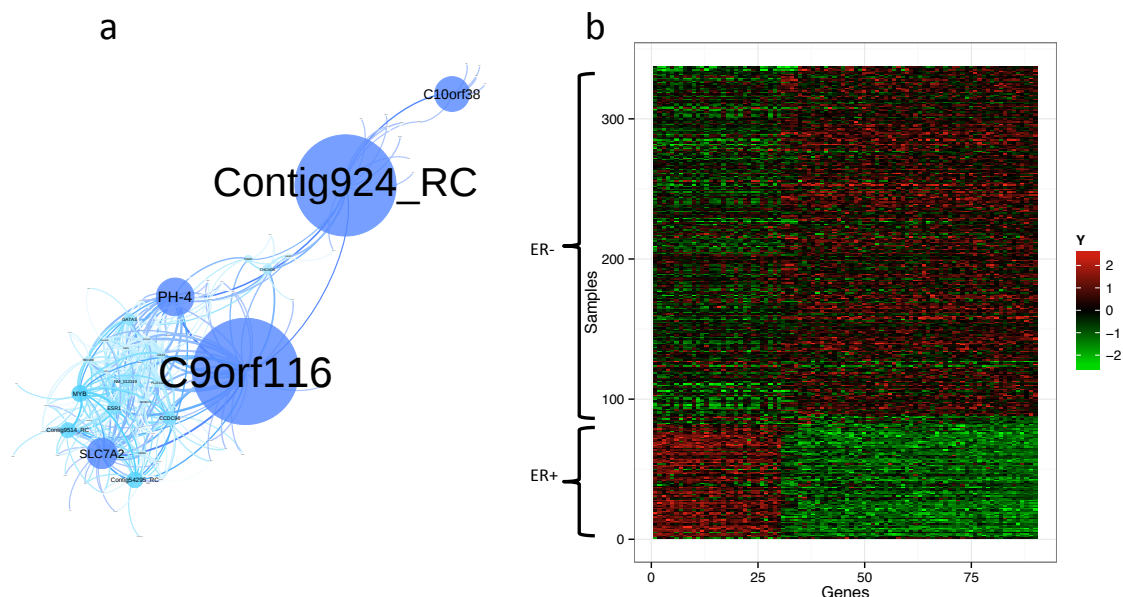


Figure 4: **Differential ER gene co-expression network and gene expression for ER differential genes.** Panel a: differential ER gene co-expression network, where node size corresponds to betweenness centrality. Panel b: gene expression levels for 90 genes in the ER differential gene co-expression network.

hypothesis, we quantified differential expression levels for the 90 genes in the original gene expression matrix (Figure 4b). We found that these genes are indeed stratified into two groups that show distinct expression patterns among the ER+ and ER- samples. In comparison, the genes in the ER-status specific co-expression networks do not show such a dramatic pattern of differential expression (Supplemental Figures S4).

In the ER differential network, we found that many of the annotated hub genes play critical roles in breast tumor development. For example, *ESR1*, one of the two genes that encodes the ER protein, is ranked 10th in this network based on the betweenness centrality criteria across all network genes, suggesting that much of the regulatory activity of tumor development is modulated by interactions with *ESR1*. *MYB* encodes the *MYB* proto-oncogene protein, a member of the *MYB* (myeloblastosis) family of transcription factors. *MYB* is highly expressed in ER+ breast tumors and tumor cell lines (Gonda *et al.*, 2008); a deficit in *MYB* activity leads to death in animals (Ramsay and Gonda, 2008). *GATA3* is a transcription factor pivotal in mediating enhancer accessibility at regulatory regions involved in *ESR1*-mediated transcription (Theodorou *et al.*, 2013) and is particularly useful as a marker for metastatic breast carcinoma (Cimino-Mathews *et al.*, 2013). *LRIG1*, the leucine-rich repeat and immunoglobulin-like domain 1, has three roles: as an *ERBB* negative regulator, as an intestinal stem cell marker, and as a tumor suppressor (Krig *et al.*, 2011; Wang *et al.*, 2013). *XBP1* is co-expressed with *ESR1* (Andres and Wittliff, 2011) and promotes triple-negative breast cancer by controlling the *HIF1 α* pathway (Chen *et al.*,

2014). *PH4* has been shown to be predictive of response in primary breast cancer patients receiving neoadjuvant chemotherapy (Bonnetterre et al., 2013).

3. Discussion

In this work, we developed a Bayesian biclustering model based on a latent factor model. We included a two-component mixture distribution to allow both sparse and dense representations of the features or samples to capture structured variation within the gene expression data. We used the regularized covariance matrix estimated from the latent factor model to build a Gaussian Markov random field with the features as nodes in the undirected network. By extracting covariance matrices corresponding to subsets of components, we were able to identify gene co-expression networks that were shared across all samples, unique to a subset of samples, or differential across sample subsets. We applied our methodology to breast tissue gene expression samples and recovered co-expression networks that are differential across ER+ and ER- tumor types.

Factor analysis methods, including the biclustering approach presented here but extending to many other well-studied models, are statistical tools developed for exploratory analyses of the data. In this work, we have exploited the latent structure in both the factor and the loading matrix to estimate the covariance matrix that is specific to sample subsets. Here we consider tissue type and tumor types, but these methods can be used for any observed binary, categorical, integer, or continuous covariate (e.g., case-control status, batch, sex, age, EBV load).

Our results show that a number of genes are identified as part of multiple tissue-specific networks. While individual genes may overlap across networks, the interactions of those genes do not. Genes that co-occur in multiple tissue-specific networks are good candidates to test for differential function across tissues. We also will use this approach to study sexual dimorphism, extracting gene networks specific to one sex or differential across the sexes. As in this work, this will greatly improve our power to identify sex-specific trans-eQTLs using (necessarily) unmatched samples.

In this current version of this approach, extracting a covariance matrix specific to a subset of the samples is performed *post hoc*: the linear projection to the latent space is performed in a mostly unsupervised way, although sparsity does add additional structure above SFA-type approaches. As described in the Results, there are multiple categories of networks that we recover. These categories include: gene networks that exist across tissues, gene networks that are unique to specific tissues, gene networks that are specific to specific subsets of samples (e.g., tumor types), and gene networks that exist across multiple tissues but are differentially co-expressed in those tissues. However, this approach is restrictive in that a covariate of interest does not directly inform the projection. Indirectly, we see that the sparsity structure on the samples allows small subsets of the samples to inform projection, but this still relies on a post hoc interpretation of those sample subsets to recover specific network types. Furthermore, it may be the case that, for the covariate we are interested in (e.g., age, sex), we do not see sufficient signal that is uniquely attributable to those samples (e.g., female) to identify a covariance matrix corresponding to the values of interest. We are currently extending this approach so that the linear projection is explicitly informed by the covariate of interest.

4. Methods

We extend the following factor analysis model

$$\mathbf{Y} = \mathbf{\Lambda}\mathbf{X} + \boldsymbol{\epsilon} \quad (4)$$

where $\mathbf{Y} \in \mathbb{R}^{p \times n}$ is the matrix of observed variables, $\mathbf{\Lambda} \in \mathbb{R}^{p \times K}$ is the loading matrix, $\mathbf{X} \in \mathbb{R}^{K \times n}$ is the factor matrix, and $\boldsymbol{\epsilon} \in \mathbb{R}^{p \times n}$ is the residual error matrix. We assume $\epsilon_{:,i} \sim \mathcal{N}(0, \boldsymbol{\Psi})$ for $i = 1, \dots, n$, where $\boldsymbol{\Psi} = \text{diag}(\psi_1, \dots, \psi_p)$.

In previous work (Gao and Engelhardt, 2012; Gao et al., 2013), a three parameter beta (\mathcal{TPB}) (Armagan et al., 2011) prior was used to model the variance of $\mathbf{\Lambda}$. Here we use \mathcal{TPB} to induce flexible shrinkage to both $\mathbf{\Lambda}$ and \mathbf{X} . Specifically, we induce three layers of shrinkage—global, factor specific, and local—to both the factors and the loadings. Below, we describe the model structure for $\mathbf{\Lambda}$; \mathbf{X} has a prior structure identical to $\mathbf{\Lambda}$ (for complete details see Appendix A).

The hierarchical structure for $\mathbf{\Lambda}$ is written as

$$\begin{aligned} \varrho &\sim \mathcal{TPB}(e, f, \nu), & \zeta_k &\sim \mathcal{TPB}(c, d, \frac{1}{\varrho} - 1) \\ \varphi_{i,k} &\sim \mathcal{TPB}(a, b, \frac{1}{\zeta_k} - 1), & \Lambda_{i,k} &\sim \mathcal{N}(0, \frac{1}{\varphi_{i,k}} - 1). \end{aligned} \quad (5)$$

Making the substitution $\eta = \frac{1}{\varrho} - 1$, $\phi_k = \frac{1}{\zeta_k} - 1$, $\theta_{i,k} = \frac{1}{\varphi_{i,k}} - 1$ we get the equivalent hierarchical structure (Armagan et al., 2011):

$$\begin{aligned} \gamma &\sim \mathcal{Ga}(f, \nu), & \eta &\sim \mathcal{Ga}(e, \gamma), & \tau_k &\sim \mathcal{Ga}(d, \eta), & \phi_k &\sim \mathcal{Ga}(c, \tau_k) \\ \delta_{i,k} &\sim \mathcal{Ga}(b, \phi_k), & \theta_{i,k} &\sim \mathcal{Ga}(a, \delta_{i,k}) & \Lambda_{i,k} &\sim \mathcal{N}(0, \theta_{i,k}). \end{aligned} \quad (6)$$

We write the i^{th} row of $\mathbf{\Lambda}$ as a multivariate Gaussian distribution,

$$\Lambda_i \sim \mathcal{N}(0, \boldsymbol{\Theta}_i) \quad (7)$$

where $\boldsymbol{\Theta}_i = \text{diag}(\theta_{i,1}, \theta_{i,2}, \dots, \theta_{i,K})$. We applied a two-component mixture model to jointly model sparse and dense effects by letting $\theta_{i,k}$ be generated from a mixture of sparse and dense components:

$$\theta_{i,k} \sim \pi \mathcal{Ga}(a, \delta_{i,k}) + (1 - \pi) \delta(\phi_k), \quad (8)$$

where the hidden variable Z_k indicates whether the loading is sparse (0) or dense (1) and has a beta Bernoulli distribution:

$$\pi | \alpha, \beta \sim \text{Be}(\alpha, \beta) \quad (9)$$

$$Z_k | \pi \sim \text{Bern}(\pi), \quad k = \{1, \dots, K\}. \quad (10)$$

A variational EM (VEM) algorithm was constructed for fast inference of the parameters (Appendix A); a Markov chain Monte Carlo approach was developed to propose initial states for VEM (Appendix B).

Acknowledgments

The authors would like to acknowledge the GTEx Consortium members for useful feedback. CG, SZ, and BEE were funded by NIH R00 HG006265 and NIH R01 MH101822. CDB was funded by NIH R01 MH101822. All code is available at the websites of CG and BEE.

Appendix A.

The complete biclustering model for BicMix

We consider the following factor analysis model:

$$\mathbf{Y} = \mathbf{\Lambda}\mathbf{X} + \boldsymbol{\epsilon}, \quad (11)$$

where $\mathbf{Y} \in \mathbb{R}^{p \times n}$ is the matrix of observed variables, $\mathbf{\Lambda} \in \mathbb{R}^{p \times K}$ is the loading matrix, $\mathbf{X} \in \mathbb{R}^{K \times n}$ is the factor matrix, and $\boldsymbol{\epsilon} \in \mathbb{R}^{p \times n}$ is the residual error matrix for p genes and n samples. We assume $\epsilon_{.,j} \sim \mathcal{N}(0, \boldsymbol{\Psi})$, where $\boldsymbol{\Psi} = \text{diag}(\psi_1, \dots, \psi_p)$.

In previous work (Gao and Engelhardt, 2012; Gao et al., 2013), a three parameter beta (\mathcal{TPB}) (Armagan et al., 2011) prior was used to model the variance of $\mathbf{\Lambda}$. The three parameter distribution has the form of

$$f(x : a, b, \phi) = \frac{\Gamma(a+b)}{\Gamma(a)\Gamma(b)} \phi^b x^{b-1} (1-x)^{a-1} \{1 + (\phi-1)x\}^{-(a+b)}, \quad (12)$$

for $x \in (0, 1)$, $a > 0$, $b > 0$ and $\phi > 0$.

Here we use \mathcal{TPB} to induce flexible shrinkage to both $\mathbf{\Lambda}$ and \mathbf{X} . Specifically, we induce three layers of shrinkage—global, factor specific and local—for both the factors and the loadings. Below, we describe the model structure for $\mathbf{\Lambda}$ and \mathbf{X} .

Hierarchical structure for $\mathbf{\Lambda}$

The hierarchical structure for $\mathbf{\Lambda}$ is written as

$$\varrho \sim \mathcal{TPB}(e, f, \nu), \quad (13)$$

$$\zeta_k \sim \mathcal{TPB}(c, d, \frac{1}{\varrho} - 1) \quad (14)$$

$$\varphi_{i,k} \sim \mathcal{TPB}(a, b, \frac{1}{\zeta_k} - 1), \quad (15)$$

$$\Lambda_{i,k} \sim \mathcal{N}(0, \frac{1}{\varphi_{i,k}} - 1). \quad (16)$$

We use the fact that

$$\varphi \sim \mathcal{TPB}(a, b, \nu) \Leftrightarrow \frac{\theta}{\nu} \sim Be'(a, b) \Leftrightarrow \theta \sim \mathcal{Ga}(a, \delta) \text{ and } \delta \sim \mathcal{Ga}(b, \nu), \quad (17)$$

where $Be'(a, b)$ and \mathcal{Ga} indicate an inverse beta and a gamma distribution, respectively. Making the substitution $\eta = \frac{1}{\varrho} - 1$, $\phi_k = \frac{1}{\zeta_k} - 1$, $\theta_{i,k} = \frac{1}{\varphi_{i,k}} - 1$, we get the equivalent hierarchical structure (Armagan et al., 2011):

$$\gamma \sim \mathcal{Ga}(f, \nu), \quad (18)$$

$$\eta \sim \mathcal{Ga}(e, \gamma), \quad (19)$$

$$\tau_k \sim \mathcal{Ga}(d, \eta), \quad (20)$$

$$\phi_k \sim \mathcal{Ga}(c, \tau_k), \quad (21)$$

$$\delta_{i,k} \sim \mathcal{Ga}(b, \phi_k), \quad (22)$$

$$\theta_{i,k} \sim \mathcal{Ga}(a, \delta_{i,k}), \quad (23)$$

$$\Lambda_{i,k} \sim \mathcal{N}(0, \theta_{i,k}). \quad (24)$$

We applied a two-component mixture model to jointly model possibly dense confounding effects by letting $\theta_{i,k}$ be generated from a mixture of sparse and dense components:

$$\theta_{i,k} \sim \pi \mathcal{G}a(a, \delta_{i,k}) + (1 - \pi) \delta(\phi_k), \quad (25)$$

where the hidden variable Z_k , which indicates whether or not the loading is sparse (1) or dense (0), is generated from the following beta Bernoulli distribution:

$$\pi | \alpha, \beta \sim Be(\alpha, \beta) \quad (26)$$

$$Z_k | \pi \sim \text{Bern}(\pi), \quad k = \{1, \dots, K\}. \quad (27)$$

Hierarchical structure for \mathbf{X}

Similarly, the hierarchical structure for \mathbf{X} is:

$$\varphi \sim \mathcal{G}a(f_X, \xi), \quad (28)$$

$$\chi \sim \mathcal{G}a(e_X, \varphi), \quad (29)$$

$$\kappa_k \sim \mathcal{G}a(d_X, \chi), \quad (30)$$

$$\omega_k \sim \mathcal{G}a(c_X, \kappa_k) \quad (31)$$

$$\rho_{k,j} \sim \mathcal{G}a(b_X, \omega_k), \quad (32)$$

$$\sigma_{k,j} \sim \pi \mathcal{G}a(a_X, \rho_{k,j}) + (1 - \pi) \delta(\omega_k) \quad (33)$$

$$x_{k,j} \sim \mathcal{N}(0, \sigma_{i,k}) \quad (34)$$

with $\sigma_{k,j}$ being generated from a two component mixture. Here, the hidden variable O_k , which indicates whether or not the factor is sparse (1) or dense (0), is generated from the following beta Bernoulli distribution:

$$\pi_X | \alpha_X, \beta_X \sim Be(\alpha_X, \beta_X) \quad (35)$$

$$O_k | \pi_X \sim \text{Bern}(\pi_X), \quad k = \{1, \dots, K\}. \quad (36)$$

Variational expectation maximization

Extending previous work ([Gao et al., 2013](#)), the posterior probability $\mathcal{P} = p(\mathbf{\Lambda}, \mathbf{X}, \mathbf{Z}, \mathbf{O}, \mathbf{\Theta} | \mathbf{Y})$ is written as:

$$\begin{aligned} \mathcal{P} &\propto p(\mathbf{Y} | \mathbf{\Lambda}, \mathbf{X}) p(\mathbf{\Lambda} | \mathbf{Z}, \mathbf{\Theta}_{\mathbf{\Lambda}}) p(\mathbf{X} | \mathbf{O}, \mathbf{\Theta}_{\mathbf{X}}) p(\mathbf{Z} | \mathbf{\Theta}_{\mathbf{\Lambda}}) p(\mathbf{O} | \mathbf{\Theta}_{\mathbf{X}}) p(\mathbf{\Theta}_{\mathbf{\Lambda}}) p(\mathbf{\Theta}_{\mathbf{X}}) \\ &\propto p(\mathbf{Y} | \mathbf{\Lambda}, \mathbf{X}) \mathcal{P}(\mathbf{\Lambda}) \mathcal{P}(\mathbf{X}), \end{aligned} \quad (37)$$

where we have used Θ_Λ and Θ_X to denote the set of parameters related to Λ and \mathbf{X} respectively. Then,

$$\begin{aligned}
\mathcal{P}(\Lambda) &= p(\Lambda|\mathbf{Z}, \Theta_\Lambda)p(\mathbf{Z}|\Theta_\Lambda)p(\Theta_\Lambda) \\
&= \left[\prod_{i=1}^p \prod_{k=1}^K \mathcal{N}(\Lambda_{i,k}|\theta_{i,k})\mathcal{G}a(\theta_{i,k}|a, \delta_{i,k})\mathcal{G}a(\delta_{i,k}|b, \phi_k) \right]^{\mathbb{1}_{Z_k=1}} \\
&\times \left[\prod_{i=1}^p \prod_{k=1}^K \mathcal{N}(\Lambda_{i,k}|\phi_k) \right]^{\mathbb{1}_{Z_k=0}} \left[\prod_{k=1}^K \mathcal{B}ern(Z_k|\pi) \right] \mathcal{B}eta(\pi|\alpha, \beta) \\
&\times \left[\prod_{k=1}^K \mathcal{G}a(\phi_k|c, \tau_k)\mathcal{G}a(\tau_k|d, \eta) \right] \mathcal{G}a(\eta|e, \gamma)\mathcal{G}a(\gamma|f, \nu)
\end{aligned} \tag{38}$$

and

$$\begin{aligned}
\mathcal{P}(\mathbf{X}) &= p(\mathbf{X}|\mathbf{O}, \Theta_X)p(\mathbf{O}|\Theta_X)p(\Theta_X) \\
&= \left[\prod_{k=1}^K \prod_{j=1}^n \mathcal{N}(x_{k,j}|\sigma_{k,j})\mathcal{G}a(\sigma_{k,j}|a_X, \rho_{k,j})\mathcal{G}a(\rho_{k,j}|b_X, \omega_k) \right]^{\mathbb{1}_{O_k=1}} \\
&\times \left[\prod_{k=1}^K \prod_{j=1}^n \mathcal{N}(x_{k,j}|\omega_k) \right]^{\mathbb{1}_{O_k=0}} \left[\prod_{k=1}^K \mathcal{B}ern(o_k|\pi_X) \right] \mathcal{B}eta(\pi_X|\alpha_X, \beta_X) \\
&\times \left[\prod_{k=1}^K \mathcal{G}a(\omega_k|c_X, \kappa_k)\mathcal{G}a(\kappa_k|d_X, \chi) \right] \mathcal{G}a(\chi|e_X, \varphi)\mathcal{G}a(\varphi|f_X, \xi)
\end{aligned} \tag{39}$$

Parameters specific to Λ

To derive the variational EM algorithm, we expand the posterior probability (Equation (18)) and write the expected complete log likelihood for parameters related to Λ , $Q(\Theta_\Lambda) =$

$\langle \ell_c(\Theta_\Lambda, \Lambda | \mathbf{Z}, \mathbf{X}, \mathbf{Y}) \rangle$ as:

$$\begin{aligned}
 Q(\Theta_\Lambda) &\propto \sum_{i=1}^p \sum_{j=1}^n \langle \log p(y_{i,j} | \Lambda, \mathbf{X}, \Theta_\Lambda, \mathbf{Z}) \rangle \\
 &+ \sum_{i=1}^p \sum_{k=1}^K \langle p(Z_k | \Theta_\Lambda) \log p(\Lambda_{i,k} | \Theta_\Lambda, Z_k) \rangle + \log p(\Theta_\Lambda) \\
 &\propto -\frac{p}{2} \ln |\Psi| - \sum_{i=1}^p \sum_{j=1}^n \frac{\left(y_{i,j} - \sum_{k=1}^K \Lambda_{i,k} \langle x_{k,j} \rangle \right)^2}{2\psi_{i,i}} + \sum_{i=1}^p \sum_{k=1}^K \langle 1 - z_k \rangle \left\{ -\frac{1}{2} \ln \phi_k - \frac{\Lambda_{i,k}^2}{2\phi_k} \right\} \\
 &+ \sum_{i=1}^p \sum_{k=1}^K \langle z_k \rangle \left\{ -\frac{1}{2} \ln \theta_{i,k} - \frac{\Lambda_{i,k}^2}{2\theta_{i,k}} + a \ln \delta_{i,k} + (a-1) \ln \theta_{i,k} - \delta_{i,k} \theta_{i,k} \right\} \\
 &+ \sum_{i=1}^p \sum_{k=1}^K \langle z_k \rangle \{ b \ln \phi_k + (b-1) \ln \delta_{i,k} - \phi_k \delta_{i,k} \} + \sum_{k=1}^K \{ \langle z_k \rangle \ln \pi + (1 - \langle z_k \rangle) \ln(1 - \pi) \} \\
 &+ \sum_{k=1}^K \{ c \ln \tau_k + (c-1) \ln \phi_k - \tau_k \phi_k + d \ln \eta + (d-1) \ln \tau_k - \eta \tau_k \} \\
 &+ e \ln \gamma + (e-1) \ln \eta - \gamma \eta + f \ln \nu + (f-1) \ln \gamma - \nu \gamma + \alpha \ln \pi + \beta \ln(1 - \pi)
 \end{aligned} \tag{40}$$

where we have used $\langle X \rangle$ to represent the expected value of X .

We obtain the MAP estimates $\hat{\Theta}_\Lambda = \arg \max_{\Theta_\Lambda} Q(\Theta_\Lambda)$. Specifically, we solve equation $\frac{\partial Q(\Theta_\Lambda)}{\partial \Theta_\Lambda} = 0$ to find the closed form of their MAP estimates. The MAP estimate for the i th row of Λ , $\Lambda_{i,\cdot}$, in matrix form is:

$$\hat{\Lambda}_{i,\cdot} = Y_{i,\cdot} \Psi_{i,i}^{-1} \mathbf{X}^T \left(\langle \mathbf{X} \Psi_{i,i}^{-1} \mathbf{X}^T \rangle + \langle \mathbf{Z} \rangle \Theta_i^{-1} + (\mathbf{I} - \langle \mathbf{Z} \rangle) \Phi^{-1} \right)^{-1} \tag{41}$$

where

$$\Theta_i = \begin{pmatrix} \theta_{i,1} & 0 & \cdots & 0 \\ 0 & \theta_{i,2} & \cdots & 0 \\ \vdots & \vdots & \ddots & \vdots \\ 0 & 0 & \cdots & \theta_{i,k} \end{pmatrix}, \quad \Phi = \begin{pmatrix} \phi_1 & 0 & \cdots & 0 \\ 0 & \phi_2 & \cdots & 0 \\ \vdots & \vdots & \ddots & \vdots \\ 0 & 0 & \cdots & \phi_k \end{pmatrix}, \tag{42}$$

and

$$\langle \mathbf{Z} \rangle = \begin{pmatrix} \langle z_1 \rangle & 0 & \cdots & 0 \\ 0 & \langle z_2 \rangle & \cdots & 0 \\ \vdots & \vdots & \ddots & \vdots \\ 0 & 0 & \cdots & \langle z_k \rangle \end{pmatrix} \tag{43}$$

and \mathbf{I} is the identity matrix.

Parameter $\theta_{i,k}$ has a generalized inverse Gaussian conditional probability (Gao et al., 2013; Armagan et al., 2011), and its MAP estimate is

$$\hat{\theta}_{i,k} = \frac{2a - 3 + \sqrt{(2a - 3)^2 + 8\Lambda_{i,k}^2 \delta_{i,k}}}{4\delta_{i,k}} \tag{44}$$

The MAP estimate for $\delta_{i,k}$ is:

$$\hat{\delta}_{i,k} = \frac{a + b - 1}{\theta_{i,k} + \phi_k} \quad (45)$$

Parameter ϕ_k generates both the sparse and dense components, and its MAP estimate takes the form of

$$\hat{\phi}_k = \frac{H + \sqrt{H^2 + MT}}{M} \quad (46)$$

where

$$H = pb\langle z_k \rangle + c - 1 - \frac{p}{2}(1 - \langle z_k \rangle) \quad (47)$$

$$M = 2 \left(\langle z_k \rangle \sum_{i=1}^p \delta_{i,k} + \tau_k \right) \quad (48)$$

$$T = \sum_{i=1}^p \Lambda_{i,k}^2. \quad (49)$$

The following parameters have similar updates to $\delta_{i,k}$, which have natural forms because of conjugacy:

$$\hat{\tau}_k = \frac{c + d - 1}{\phi_k + \eta} \quad (50)$$

$$\hat{\eta} = \frac{Kd + e - 1}{\gamma + \sum_k \tau_k} \quad (51)$$

$$\hat{\gamma} = \frac{e + f - 1}{\eta + \nu} \quad (52)$$

The expected value of $Z_k | \Theta$ is computed as:

$$\langle z_k | \Theta_\Lambda \rangle = p(Z_k = 1 | \Theta_\Lambda) \quad (53)$$

$$= \frac{\pi \prod_{i=1}^p \mathcal{N}(\Lambda_{i,k} | \theta_{i,k}) \mathcal{G}a(\theta_{i,k} | a, \delta_{i,k}) \mathcal{G}a(\delta_{i,k} | b, \phi_k)}{(1 - \pi) \left(\prod_{i=1}^p \mathcal{N}(\Lambda_{i,k} | \phi_k) \right) + \pi \prod_{i=1}^p \mathcal{N}(\Lambda_{i,k} | \theta_{i,k}) \mathcal{G}a(\theta_{i,k} | a, \delta_{i,k}) \mathcal{G}a(\delta_{i,k} | b, \phi_k)} \text{notag} \quad (54)$$

The prior on the indicator variable for sparse and dense components, π , has a beta distribution, and its geometric mean is the following:

$$\langle \ln \pi \rangle = \psi \left(\sum_{k=1}^K \langle z_k \rangle + \alpha \right) - \psi(K + \alpha + \beta) \quad (55)$$

where ψ is the digamma function.

Parameters specific to \mathbf{X}

Similarly, the expected complete log likelihood for parameters related to \mathbf{X} takes the following form:

$$\begin{aligned}
 Q(\Theta_X) &\propto \sum_{i=1}^p \sum_{j=1}^n \langle \log p(y_{i,j} | \Lambda, \mathbf{X}, \Theta_X, \mathbf{O}) \rangle \\
 &+ \sum_{k=1}^K \sum_{j=1}^n \langle p(O_k | \Theta_X) \log p(X_{k,j} | \Theta_X, O_k) \rangle + \log p(\Theta_X) \\
 &\propto -\frac{p}{2} \ln |\Psi| - \sum_{i=1}^p \sum_{j=1}^n \frac{\left(y_{i,j} - \sum_{k=1}^K \Lambda_{i,k} \langle x_{k,j} \rangle \right)^2}{2\psi_{i,i}} + \sum_{k=1}^K \sum_{j=1}^n \langle 1 - o_k \rangle \left\{ -\frac{1}{2} \ln \omega_k - \frac{\langle x_{k,j}^2 \rangle}{2\omega_k} \right\} \\
 &+ \sum_{k=1}^K \sum_{j=1}^n \langle o_k \rangle \left\{ -\frac{1}{2} \ln \sigma_{k,j} - \frac{\langle x_{k,j}^2 \rangle}{2\sigma_{k,j}} + a_X \ln \rho_{k,j} + (a_X - 1) \ln \sigma_{k,j} - \rho_{k,j} \sigma_{k,j} \right\} \\
 &+ \sum_{k=1}^K \sum_{j=1}^n \langle o_k \rangle \{ b_X \ln \omega_k + (b_X - 1) \ln \rho_{k,j} - \omega_k \rho_{k,j} \} + \sum_{k=1}^K \{ \langle o_k \rangle \ln \pi_X + (1 - \langle o_k \rangle) \ln(1 - \pi_X) \} \\
 &+ \sum_{k=1}^K \{ c_X \ln \kappa_k + (c_X - 1) \ln \omega_k - \kappa_k \omega_k + d_X \ln \chi + (d_X - 1) \ln \kappa_k - \chi \kappa_k \} \\
 &+ e_X \ln \varphi + (e_X - 1) \ln \chi - \varphi \chi + f_X \ln \xi + (f_X - 1) \ln \varphi - \xi \varphi + \alpha_X \ln \pi_X + \beta_X \ln(1 - \pi_X)
 \end{aligned} \tag{56}$$

To simplify the calculation, we assumed that the joint distribution $p(o_k, x_{k,j})$ factorizes to $p(o_k)p(x_{k,j})$.

The closed form solutions for the parameters related to \mathbf{X} are:

$$\langle \mathbf{X}_{\cdot,j} \rangle = (\Lambda^T \Psi^{-1} \Lambda + \langle \mathbf{O} \rangle \Sigma_j^{-1} + (\mathbf{I} - \langle \mathbf{O} \rangle) \Omega^{-1})^{-1} \Lambda^T \Psi^{-1} Y_{\cdot,j}, \tag{57}$$

where

$$\Sigma_j = \begin{pmatrix} \sigma_{1,j} & 0 & \cdots & 0 \\ 0 & \sigma_{2,j} & \cdots & 0 \\ \vdots & \vdots & \ddots & \vdots \\ 0 & 0 & \cdots & \sigma_{k,j} \end{pmatrix}, \quad \Omega = \begin{pmatrix} \omega_1 & 0 & \cdots & 0 \\ 0 & \omega_2 & \cdots & 0 \\ \vdots & \vdots & \ddots & \vdots \\ 0 & 0 & \cdots & \omega_k \end{pmatrix}, \tag{58}$$

and

$$\mathbf{O} = \begin{pmatrix} \langle o_1 \rangle & 0 & \cdots & 0 \\ 0 & \langle o_2 \rangle & \cdots & 0 \\ \vdots & \vdots & \ddots & \vdots \\ 0 & 0 & \cdots & \langle o_k \rangle \end{pmatrix} \tag{59}$$

In these equations,

$$\hat{\sigma}_{k,j} = \frac{2a_X - 3 + \sqrt{(2a_X - 3)^2 + 8 \langle x_{k,j}^2 \rangle \rho_{k,j}}}{4\rho_{k,j}}, \quad (60)$$

$$\hat{\rho}_{k,j} = \frac{a_X + b_X - 1}{\sigma_{k,j} + \omega_k}, \quad (61)$$

$$\hat{\omega}_k = \frac{H + \sqrt{H^2 + MT}}{M}, \quad (62)$$

where

$$H = nb_X \langle o_k \rangle + c_X - 1 - \frac{n}{2}(1 - \langle o_k \rangle) \quad (63)$$

$$M = 2 \left(\langle o_k \rangle \sum_{j=1}^n \rho_{k,j} + \kappa_k \right) \quad (64)$$

$$T = \sum_{j=1}^n \langle x_{k,j}^2 \rangle. \quad (65)$$

We also need to compute the expected value of $\mathbf{X}\Psi_{i,i}^{-1}\mathbf{X}^T$:

$$\langle \mathbf{X}\Psi_{i,i}^{-1}\mathbf{X}^T \rangle = \Psi_{i,i}^{-1} \left(\langle \mathbf{X} \rangle \langle \mathbf{X} \rangle^T + \Sigma_X \right) \quad (66)$$

where Σ_X denotes the covariance matrix of \mathbf{X} .

Finally:

$$\hat{\kappa}_k = \frac{c_X + d_X - 1}{\omega_k + \chi} \quad (67)$$

$$\hat{\chi} = \frac{Kd_X + e_X - 1}{\varphi + \sum_k \kappa_k} \quad (68)$$

$$\hat{\varphi} = \frac{e_X + f_X - 1}{\chi + \xi}. \quad (69)$$

Now we consider the parameters O_k :

$$\langle O_k | \Theta_X \rangle = p(O_k = 1 | \Theta_X) \quad (70)$$

$$= \frac{\pi \prod_{j=1}^n \mathcal{N}(X_{k,j} | \sigma_{k,j}) \mathcal{G}a(\sigma_{k,j} | a_X, \rho_{k,j}) \mathcal{G}a(\rho_{k,j} | b_X, \omega_k)}{(1 - \pi) \left(\prod_{j=1}^n \mathcal{N}(X_{k,j} | \omega_k) \right) + \pi \prod_{j=1}^n \mathcal{N}(X_{k,j} | \sigma_{k,j}) \mathcal{G}a(\sigma_{k,j} | a_X, \rho_{k,j}) \mathcal{G}a(\rho_{k,j} | b_X, \omega_k)}.$$

$$\langle \ln \pi_X \rangle = \psi \left(\sum_{k=1}^K \langle o_k \rangle + \alpha_X \right) - \psi(K + \alpha_X + \beta_X) \quad (71)$$

and finally, assuming that the residual precision has a conjugate prior, $\frac{1}{\Psi_{i,i}} \sim \mathcal{G}a(1, 1)$, then we have

$$\Psi = \text{diag} \left(\frac{\mathbf{Y}\mathbf{Y}^T - 2\mathbf{Y} \langle \mathbf{X}^T \rangle \boldsymbol{\Lambda}^T + \boldsymbol{\Lambda} \langle \mathbf{X}\mathbf{X}^T \rangle \boldsymbol{\Lambda}^T + 2\mathbf{I}}{n + 2} \right). \quad (72)$$

VEM algorithm

To summarize the description above, we write the complete VEM algorithm for parameter updates:

Algorithm 1: Variational expectation maximization for BicMix

Data: $p \times n$ Gene expression matrix, K , n_itr

Result: $p \times K$ and $K \times n$ matrices with mixture of sparse and dense components

begin

Initialize starting values:

$a, b, c, d, e, f, a_X, b_X, c_X, d_X, e_X, f_X \leftarrow 0.5$

$\alpha, \beta, \alpha_X, \beta_X \leftarrow 1$

 Sample $\eta, \gamma, \chi, \varphi \leftarrow \mathcal{G}a(1, 1)$

 Sample $\pi \leftarrow \mathcal{B}eta(\alpha, \beta)$, $\pi_X \leftarrow \mathcal{B}eta(\alpha_X, \beta_X)$,

for $i \leftarrow 1$ **to** p **do**

\lfloor Sample $\psi_{i,i} \leftarrow \mathcal{G}a(1, 1)$

for $k \leftarrow 1$ **to** K **do**

 Sample $z_k \leftarrow \mathcal{B}ern(\pi)$, $o_k \leftarrow \mathcal{B}ern(\pi_X)$

 Sample $\phi_k, \tau_k, \omega_k, \kappa_k \leftarrow \mathcal{G}a(1, 1)$

for $i \leftarrow 1$ **to** p **do**

\lfloor Sample $\Lambda_{i,k} \leftarrow \mathcal{N}(0, 1)$, Sample $\theta_{i,k}, \delta_{i,k} \leftarrow \mathcal{G}a(1, 1)$

for $j \leftarrow 1$ **to** n **do**

\lfloor Sample $X_{k,j} \leftarrow \mathcal{N}(0, 1)$, Sample $\sigma_{k,j}, \rho_{k,j} \leftarrow \mathcal{N}(0, 1)$

Begin iterations:

for $t \leftarrow 1$ **to** n_itr **do**

Update parameters that are specific to Λ :

for $i \leftarrow 1$ **to** p **do**

 Update $\Lambda_{i,\cdot} \leftarrow$ equation (41)

for $k \leftarrow 1$ **to** K **do**

\lfloor Update $\theta_{i,k} \leftarrow$ equation (44), $\delta_{i,k} \leftarrow$ equation (45)

for $k \leftarrow 1$ **to** K **do**

\lfloor Update $\phi_k \leftarrow$ equation (46), $\tau_k \leftarrow$ equation (50), $z_k \leftarrow$ equation (53)

 Update $\eta \leftarrow$ equation (51), $\gamma \leftarrow$ equation (52), $\pi \leftarrow$ equation (55)

Update parameters that are specific to \mathbf{X} :

for $j \leftarrow 1$ **to** n **do**

 Update $X_{\cdot,j} \leftarrow$ equation (57)

for $k \leftarrow 1$ **to** K **do**

\lfloor Update $\sigma_{k,j} \leftarrow$ equation (60), $\rho_{k,j} \leftarrow$ equation (61)

for $k \leftarrow 1$ **to** K **do**

\lfloor Update $\omega_k \leftarrow$ equation (62), $\kappa_k \leftarrow$ equation (67), $o_k \leftarrow$ equation (70)

 Update $\chi \leftarrow$ equation (68), $\varphi \leftarrow$ equation (69), $\pi_X \leftarrow$ equation (71)

for $i \leftarrow 1$ **to** p **do**

\lfloor Update $\psi_{i,i} \leftarrow$ equation (72)

 Output $\Lambda, \mathbf{X}, Z, O$

Appendix B.

MCMC: conditional distributions of BicMix parameters

We derive below the conditional distributions that capture the MCMC approach that we implemented for BicMix. In our manuscript, we used MCMC to compute the warm start parameter settings in the simulations.

Conditional distributions for parameters related to Λ

We updated the loading matrix Λ one row at a time, where each row consists of values across the K components. The i th row of the loading matrix, $\Lambda_{i,\cdot}$, has the following posterior distribution,

$$\Lambda_{i,\cdot} | Y_i, \mathbf{X}, \Theta_i, \Psi_{i,i} \sim \mathcal{N} \left(Y_i, \Psi_{i,i}^{-1} \mathbf{X}^T \left(\mathbf{X} \Psi_{i,i}^{-1} \mathbf{X}^T + \mathbf{V}_i^{-1} \right)^{-1}, \mathbf{X} \Psi_{i,i}^{-1} \mathbf{X}^T + \mathbf{V}_i^{-1} \right) \quad (73)$$

where \mathbf{V}_i is a $K \times K$ diagonal matrix. If we use $V_{i,k,k}$ to denote the (k, k) th element for V_i , then we sample $V_{i,k,k}$ and its related parameters as follows:

$$V_{i,k,k} = \begin{cases} \theta_{i,k} & \text{if } Z_k = 1; \\ \phi_k & \text{if } Z_k = 0. \end{cases} \quad (74)$$

We sample values for the parameters conditional on sparse and dense state as follows. If $Z_k = 1$,

$$\theta_{i,k} | \Lambda_{i,k}, \delta_{i,k} \sim \mathcal{GIG} \left(a - \frac{1}{2}, 2\delta_{i,k}, \Lambda_{i,k}^2 \right) \quad (75)$$

$$\delta_{i,k} | \theta_{i,k}, \phi_k \sim \mathcal{G}a(a + b, \theta_{i,k} + \phi_k) \quad (76)$$

$$\phi_k | \delta_{i,k}, \tau_k \sim \mathcal{G}a \left(pb + c, \sum_{i=1}^p \delta_{i,k} + \tau_k \right). \quad (77)$$

If $Z_k = 0$,

$$\phi_k | \tau_k, \Lambda_{i,k} \sim \mathcal{GIG} \left(c - \frac{p}{2}, 2\tau_k, \sum_{i=1}^p \Lambda_{i,k}^2 \right). \quad (78)$$

The following parameters are not sparse or dense component specific; they each have a gamma conditional distribution because of conjugacy:

$$\tau_k | \phi_k, \eta \sim \mathcal{G}a(c + d, \phi_k + \eta) \quad (79)$$

$$\eta | \gamma, \tau_k \sim \mathcal{G}a \left(Kd + e, \gamma + \sum_{k=1}^K \tau_k \right) \quad (80)$$

$$\gamma | \eta, \nu \sim \mathcal{G}a(e + f, \eta + \nu). \quad (81)$$

The conditional probability for Z_k has a Bernoulli distribution:

$$p(Z_k = 1 | \Theta_\Lambda) = \frac{\pi \prod_{i=1}^p \mathcal{N}(\Lambda_{i,k} | \theta_{i,k}) \mathcal{G}a(\theta_{i,k} | a, \delta_{i,k}) \mathcal{G}a(\delta_{i,k} | b, \phi_k)}{(1 - \pi) \left(\prod_{i=1}^p \mathcal{N}(\Lambda_{i,k} | \phi_k) \right) + \pi \prod_{i=1}^p \mathcal{N}(\Lambda_{i,k} | \theta_{i,k}) \mathcal{G}a(\theta_{i,k} | a, \delta_{i,k}) \mathcal{G}a(\delta_{i,k} | b, \phi_k)}.$$

Let $p_Z = p(Z_k = 1 | \Theta_\Lambda)$; then the conditional probability for Z_k is

$$Z_k | p_Z \sim \text{Bern}(p_Z). \quad (82)$$

The mixing proportion π has a beta conditional probability:

$$\pi | \alpha, \beta, Z_k \sim \text{Beta} \left(\alpha + \sum_{k=1}^K \mathbf{1}_{Z_k=1}, K - \sum_{k=1}^K \mathbf{1}_{Z_k=0} + \beta \right) \quad (83)$$

where $\mathbf{1}$ is the indicator function.

Conditional distributions for parameters related to \mathbf{X}

We updated the factor matrix \mathbf{X} one column at a time, where each column consists of values across the K components; the j th column of the factor matrix, $X_{\cdot,j}$, has the following posterior distribution,

$$X_{\cdot,j} | Y_{\cdot,j}, \Lambda, \Sigma_j, \Psi \sim \mathcal{N} \left((\Lambda^T \Psi^{-1} \Lambda + \mathbf{W}_j^{-1})^{-1} \Lambda^T \Psi^{-1} Y_{\cdot,j}, \Lambda^T \Psi^{-1} \Lambda + \mathbf{W}_j^{-1} \right), \quad (84)$$

where \mathbf{W}_j is a $K \times K$ diagonal matrix. If we use $W_{j,k,k}$ to denote the (k, k) th element for \mathbf{W}_j , then we sample the value of $W_{j,k,k}$ as follows:

$$W_{j,k,k} = \begin{cases} \sigma_{k,j} & \text{if } O_k = 1; \\ \omega_k & \text{if } O_k = 0. \end{cases} \quad (85)$$

We sample the values of the parameters conditional on the sparse and dense state as follows. If $O_k = 1$

$$\sigma_{k,j} | X_{k,j}, \rho_{k,j} \sim \text{GIG} \left(a_X - \frac{1}{2}, 2\rho_{k,j}, X_{k,j}^2 \right) \quad (86)$$

$$\rho_{k,j} | \Sigma_{k,j}, \omega_k \sim \text{Ga}(a_X + b_X, \rho_{k,j} + \omega_k) \quad (87)$$

$$\omega_k | \rho_{k,j}, \omega_k \sim \text{Ga} \left(nb_X + c_X, \sum_{j=1}^n \rho_{k,j} + \omega_k \right). \quad (88)$$

If $O_k = 0$

$$\omega_k | \kappa_k, X_{k,j} \sim \text{GIG} \left(c_X - \frac{n}{2}, 2\kappa_k, \sum_{j=1}^n x_{k,j}^2 \right). \quad (89)$$

The following parameters are not sparse or dense component specific; they each have a gamma conditional distribution because of conjugacy:

$$\kappa_k \sim \text{Ga}(c_X + d_X, \omega_k + \chi) \quad (90)$$

$$\chi \sim \text{Ga} \left(Kd_X + e_X, \varphi + \sum_k \kappa_k \right) \quad (91)$$

$$\varphi \sim \text{Ga}(e_X + f_X, \chi + \xi). \quad (92)$$

The conditional probability for O_k has a Bernoulli distribution:

$$p(O_k = 1 | \Theta_X) = \frac{\pi \prod_{j=1}^n \mathcal{N}(X_{k,j} | \sigma_{k,j}) \mathcal{G}a(\sigma_{k,j} | a_X, \rho_{k,j}) \mathcal{G}a(\rho_{k,j} | b_X, \omega_k)}{(1 - \pi) \left(\prod_{j=1}^n \mathcal{N}(X_{k,j} | \omega_k) \right) + \pi \prod_{j=1}^n \mathcal{N}(X_{k,j} | \sigma_{k,j}) \mathcal{G}a(\sigma_{k,j} | a_X, \rho_{k,j}) \mathcal{G}a(\rho_{k,j} | b_X, \omega_k)}. \quad (93)$$

Let $p_X = p(O_k = 1 | \Theta_X)$; then the conditional probability for O_k is

$$O_k | p_X \sim \text{Bern}(p_X). \quad (94)$$

The mixing proportion π has a beta conditional probability:

$$\pi_X | \alpha_X, \beta_X, O_k \sim \text{Beta} \left(\alpha_X + \sum_{k=1}^K \mathbb{1}_{O_k=1}, K - \sum_{k=1}^K \mathbb{1}_{O_k=0} + \beta_X \right) \quad (95)$$

where $\mathbb{1}$ is the indicator function. Finally, we have,

$$\psi_{i,i} \sim \text{IG} \left(\frac{n}{2} + 1, \frac{\sum_{j=1}^n \left(y_{i,j} - \sum_{k=1}^K \Lambda_{i,k} x_{k,j} \right)^2}{2} + 1 \right). \quad (96)$$

MCMC for parameter estimation in BicMix

We implemented the following MCMC algorithm for sampling the parameters of the BicMix model.

Algorithm 2: MCMC algorithm for BicMix

Data: $p \times n$ Gene expression matrix, K , n_itr

Result: $p \times K$ and $K \times n$ matrices with both sparse and dense components

begin

Initialization:

Sample the initial values of the parameters as described in Section (4)

Begin iterations:

for $t \leftarrow 1$ **to** n_itr **do**

Sample parameters specific to Λ :

for $i \leftarrow 1$ **to** p **do**

for $k \leftarrow 1$ **to** K **do**

 Sample $V_{i,k,k}$ according to equation (74)

 Sample $\Lambda_{i,\cdot}$ according to equation (73)

for $k \leftarrow 1$ **to** K **do**

if $z_k = 1$ **then**

 Sample ϕ_k according to equation (77)

for $i \leftarrow 1$ **to** p **do**

 Sample $\theta_{i,k}$ according to equation (75), $\delta_{i,k}$ according to equation (76),

if $z_k = 0$ **then**

 Sample ϕ_k according to equation (78)

for $k \leftarrow 1$ **to** K **do**

 Sample τ_k according to equation (79), z_k with equation (82)

 Sample η according to equation (80), γ with equation (81), π with equation (83)

Sample parameters specific to \mathbf{X} :

for $j \leftarrow 1$ **to** n **do**

for $k \leftarrow 1$ **to** K **do**

 Sample $W_{j,k,k}$ according to equation (85)

 Sample $X_{\cdot,j}$ according to equation (84)

for $k \leftarrow 1$ **to** K **do**

if $o_k = 1$ **then**

 Sample ω_k according to equation (88)

for $j \leftarrow 1$ **to** n **do**

 Sample $\sigma_{k,j}$ according to equation (86), $\rho_{k,j}$ according to equation (87),

if $o_k = 0$ **then**

 Sample ω_k according to equation (89)

for $k \leftarrow 1$ **to** K **do**

 Sample κ_k according to equation (90), o_k according to equation (94)

 Sample χ according to equation (91), φ with equation (92), π_X with equation (95)

for $i \leftarrow 1$ **to** p **do**

 Sample $\psi_{i,i}$ according to equation (96)

Output Λ , \mathbf{X} , Z , O

Appendix C.

Data processing and comparative methods

Processing the breast cancer gene expression data

The breast cancer data set is maintained by Dana-Farber Cancer Institute at Harvard University, and is available through their R package: `breastCancerNKI` version 1.3.1 (Schroeder *et al.*, 2011). We removed genes with $> 10\%$ missing values. We imputed the remaining missing values using the R package `impute` (version 1.36.0) (Hastie *et al.*, 1999). We projected the gene expression levels of each gene to the quantiles of a standard normal. There were 24,158 genes remaining in the data set after filtering.

Simulation comparison

We compared BicMix to five other methods: Fabia, Plaid, CC, Bimax, and Spectral biclustering. We ran these methods using the following settings.

For Sim1, we set the number of components to the correct values, and ran each method as follows.

- We ran Fabia (version 2.10.2) using its default parameter settings.
- We ran Fabia-truth using default parameter settings. We set the sparsity threshold in Fabia to the number (from 100 quantiles of the uniform distribution over $[0.1, 5]$) that produced the closest match in the recovered matrices to the number of non-zero elements in the simulated data.
- We ran Plaid (implemented in the R package `biclust` (Kaiser *et al.*, 2009) version 1.0.2) using `background = TRUE` to capture the noise, maximum layers were set to 10, number of iterations to find starting values was set to 10, and the number of iterations to find the layers was set to 100.
- We ran CC (implemented in the R package `biclust` (Kaiser *et al.*, 2009) version 1.0.2) by setting maximum accepted score `delta = 1.5` and the scaling factor `alpha=1.0`.
- We ran Bimax (implemented in the R package `biclust` (Kaiser *et al.*, 2009) version 1.0.2) by setting the minimum number of rows and columns to 2.
- We ran Spectral biclustering (implemented in the R package `biclust` (Kaiser *et al.*, 2009) version 1.0.2) by setting the normalization method to `bistochastization`, the number of eigenvalues for constructing the biclusters was set to 10, and the minimum number of rows and columns for the biclusters were set to 2.

For Sim2, we corrected the simulated data for the dense components by controlling for five PCs, and we ran the methods as in Sim1, but setting the number of components to 10.

Redundancy of components

We calculated a simple statistic to check the redundancy of the multiple components obtained across multiple runs as follows. For every component across all runs, we counted

the number of genes with non-zero values, denoted as ng , and the number of samples with non-zero values, denoted as ns for each component. We then grouped the components that share the same ng and ns . For each pair of components in the same group, we counted how many components have non-zero values for the same genes and the same samples (i.e., the ℓ_0 norm). Suppose we have two components, where component 1 has loading vector L_1 and factor vector of F_1 , and component 2 has loading vector L_2 and factor vector of F_2 . We transformed L_1, L_2, F_1, F_2 to binary vectors where 1 indicates non-zero values and 0 indicate zeros values. Then the number of different genes between L_1 and L_2 is simply $ng_{dif} = \sum_{i=1}^p (L_{1,i} - L_{2,i})^2$, and the number of different samples between F_1 and F_2 is simply $ns_{dif} = \sum_{i=1}^n (F_{1,i} - F_{2,i})^2$. The redundancy corresponds to the number of pairs for which both ng and ns are zero.

Appendix D.

Algorithm for identifying gene co-expression networks from BicMix

We write out the algorithm we used to build the gene co-expression networks using the fitted BicMix model. Note that the sparsity-inducing prior on the covariance matrix of the factors increases the difficulty of computing the gene-wise covariance matrix relative to the common identity matrix covariance in the prior of the factors; however, all of the elements necessary to compute an estimate of the factor covariance matrix have been explicitly quantified in the VEM algorithm already.

Algorithm 3: Algorithm to construct gene co-expression network

Data: $p \times K$ loading matrix and $K \times n$ factor matrix; Ψ ; *net_type*, *rep*.

Result: A subset of genes

begin

```

for  $i \leftarrow 1$  to  $n\_runs$  do
  for  $k \leftarrow 1$  to  $K$  do
    /*use  $n_{gene}[i], n_{sample}[i]$  to denote the number of genes and samples with
    non-zero values in a component at iteration  $i^*$ */
    if  $n_{genes}[5000] - n_{genes}[10000] > 50$  &
     $n_{samples}[5000] - n_{samples}[10000] > 50$  then
       $\perp$  discard component  $k$ 
    if net_type = subset specific then
       $\perp$  Add component to  $A$  when non-zero factors are only in class  $c$ 
    if net_type = subset differential then
       $\perp$  Compute Wilcoxon rank sum test for non-zero factor values across classes
       $\perp$   $c, d$  Add component to  $A$  when  $p < 1 \times 10^{-10}$ 
    Construct the covariance matrix for  $\mathbf{X}$  as  $\Sigma \leftarrow \langle \mathbf{X}\mathbf{X}^T \rangle - \langle \mathbf{X} \rangle \langle \mathbf{X} \rangle^T$ 
    (Equations 66 and 57)
    Calculate the variance for the residual as  $\Psi \leftarrow$  equation (72)
    Construct the precision matrix for subset  $A$  as  $\Delta^i = \left( \Lambda_A^i \Sigma_{A,A}^i \Lambda_A^{i,T} + \Psi \right)^{-1}$ 
    Run GeneNet (Schafer and Strimmer, 2005a) on  $\Delta^i$  to test significance of
    edges
    Store edges with probability of presence  $\geq 0.8$ 
  Count number of times each edge is found across all runs
  Keep edges that are found  $\geq rep$  times
  Output the nodes and edges
  Draw graph using Gephi (Bastian et al., 2009)

```

References

Jess S. Aguilar-Ruiz. Shifting and scaling patterns from gene expression data. *Bioinformatics*, 21(20):3840–3845, October 2005. ISSN 1367-4803, 1460-2059. doi: 10.1093/bioinformatics/bti641. PMID: 16144809.

- M. Aharon, M. Elad, and A. Bruckstein. K-SVD: An Algorithm for Designing Overcomplete Dictionaries for Sparse Representation. *Signal Processing, IEEE Transactions on*, 54(11):4311–4322, November 2006. ISSN 1053-587X. doi: 10.1109/TSP.2006.881199.
- Sarah A. Andres and James L. Wittliff. Relationships of ESR1 and XBP1 expression in human breast carcinoma and stromal cells isolated by laser capture microdissection compared to intact breast cancer tissue. *Endocrine*, 40(2):212–221, October 2011. ISSN 1559-0100. doi: 10.1007/s12020-011-9522-x.
- Artin Armagan, David B. Dunson, and Merlise Clyde. Generalized beta mixtures of gaussians. In John Shawe-Taylor, Richard S. Zemel, Peter L. Bartlett, Fernando C. N. Pereira, and Kilian Q. Weinberger, editors, *NIPS*, pages 523–531, 2011.
- Mathieu Bastian, Sebastien Heymann, and Mathieu Jacomy. Gephi: An open source software for exploring and manipulating networks, 2009.
- Amir Ben-Dor, Benny Chor, Richard Karp, and Zohar Yakhini. Discovering local structure in gene expression data: The order-preserving submatrix problem. *Journal of Computational Biology*, 10(3-4):373–384, June 2003. ISSN 1066-5277, 1557-8666. doi: 10.1089/10665270360688075.
- Sven Bergmann, Jan Ihmels, and Naama Barkai. Iterative signature algorithm for the analysis of large-scale gene expression data. *Physical review. E, Statistical, nonlinear, and soft matter physics*, 67(3 Pt 1):031902, March 2003. ISSN 1539-3755. PMID: 12689096.
- A. Bhattacharya and D. B. Dunson. Sparse bayesian infinite factor models. *Biometrika*, 98(2):291–306, 2011.
- J. Bonneterre, F. Rvillion, C. Desauw, E. Blot, A. Kramar, C. Fournier, L. Hornez, and J. P. Peyrat. Plasma and tissue proteomic prognostic factors of response in primary breast cancer patients receiving neoadjuvant chemotherapy. *Oncology Reports*, 29(1):355–361, January 2013. ISSN 1791-2431. doi: 10.3892/or.2012.2090.
- Doruk Bozda?, Jeffrey D. Parvin, and Umit V. Catalyurek. A biclustering method to discover co-regulated genes using diverse gene expression datasets. In Sanguthevar Rajasekaran, editor, *Bioinformatics and Computational Biology*, number 5462 in Lecture Notes in Computer Science, pages 151–163. Springer Berlin Heidelberg, January 2009. ISBN 978-3-642-00726-2, 978-3-642-00727-9.
- Christopher D. Brown, Lara M. Mangravite, and Barbara E. Engelhardt. Integrative modeling of eQTLs and cis-regulatory elements suggests mechanisms underlying cell type specificity of eQTLs. *PLoS Genet*, 9(8):e1003649, August 2013. doi: 10.1371/journal.pgen.1003649.
- Stanislav Busygin, Oleg Prokopyev, and Panos M. Pardalos. Biclustering in data mining. *Computers & Operations Research*, 35(9):2964–2987, September 2008. ISSN 0305-0548. doi: 10.1016/j.cor.2007.01.005.

- C. M. Carvalho, J. E. Lucas, Q. Wang, J. Chang, J. R. Nevins, and M. West. High-dimensional sparse factor modelling - applications in gene expression genomics. *Journal of the American Statistical Association*, 103:1438–1456, 2008. PMID 3017385.
- Xi Chen, Dimitrios Iliopoulos, Qing Zhang, Qianzi Tang, Matthew B. Greenblatt, Maria Hatziapostolou, Elgene Lim, Wai Leong Tam, Min Ni, Yiwen Chen, Junhua Mai, Haifa Shen, Dorothy Z. Hu, Stanley Adoro, Bella Hu, Minkyung Song, Chen Tan, Melissa D. Landis, Mauro Ferrari, Sandra J. Shin, Myles Brown, Jenny C. Chang, X. Shirley Liu, and Laurie H. Glimcher. XBP1 promotes triple-negative breast cancer by controlling the HIF1 α pathway. *Nature*, 508(7494):103–107, April 2014. ISSN 0028-0836. doi: 10.1038/nature13119.
- Y Cheng and G M Church. Biclustering of expression data. *Proceedings / ... International Conference on Intelligent Systems for Molecular Biology ; ISMB. International Conference on Intelligent Systems for Molecular Biology*, 8:93–103, 2000. ISSN 1553-0833. PMID: 10977070.
- Ashley Cimino-Mathews, Andrea P. Subhawong, Peter B. Illei, Rajni Sharma, Marc K. Halushka, Russell Vang, John H. Fetting, Ben Ho Park, and Pedram Argani. GATA3 expression in breast carcinoma: utility in triple-negative, sarcomatoid, and metastatic carcinomas. *Human Pathology*, 44(7):1341–1349, July 2013. ISSN 1532-8392. doi: 10.1016/j.humpath.2012.11.003.
- Maria I. Davidich and Stefan Bornholdt. Boolean network model predicts cell cycle sequence of fission yeast. *PLoS ONE*, 3(2):e1672, February 2008. doi: 10.1371/journal.pone.0001672.
- P.A.D. de Castro, F.O. de Franga, H.M. Ferreira, and F.J. Von Zuben. Evaluating the performance of a biclustering algorithm applied to collaborative filtering - a comparative analysis. In *7th International Conference on Hybrid Intelligent Systems, 2007. HIS 2007*, pages 65–70, September 2007. doi: 10.1109/HIS.2007.55.
- Michael B. Eisen, Paul T. Spellman, Patrick O. Brown, and David Botstein. Cluster analysis and display of genome-wide expression patterns. *Proceedings of the National Academy of Sciences*, 95(25):14863–14868, December 1998. ISSN 0027-8424, 1091-6490.
- Barbara Engelhardt and Matthew Stephens. Analysis of population structure: A unifying framework and novel methods based on sparse factor analysis. *PLoS Genetics*, 6(9): e1001117, 2010.
- Kemal Eren, Mehmet Deveci, Onur Kktun, and mit V. atalyrek. A comparative analysis of biclustering algorithms for gene expression data. *Briefings in Bioinformatics*, page bbs032, July 2012. ISSN 1467-5463, 1477-4054. doi: 10.1093/bib/bbs032. PMID: 22772837.
- N. Friedman, M. Linial, I. Nachman, and D. Pe’er. Using bayesian networks to analyze expression data. *Journal of Computational Biology: A Journal of Computational Molecular Cell Biology*, 7(3-4):601–620, 2000. ISSN 1066-5277. doi: 10.1089/106652700750050961.

- C. Gao and BE. Engelhardt. A sparse factor analysis model for high dimensional latent spaces. *NIPS: Workshop on Analysis Operator Learning vs. Dictionary Learning: Fraternal Twins in Sparse Modeling*, 2012.
- C. Gao, C. D Brown, and B. E Engelhardt. A latent factor model with a mixture of sparse and dense factors to model gene expression data with confounding effects. *ArXiv e-prints*, October 2013.
- Thomas J. Gonda, Paul Leo, and Robert G. Ramsay. Estrogen and MYB in breast cancer: potential for new therapies. *Expert Opinion on Biological Therapy*, 8(6):713–717, June 2008. ISSN 1744-7682. doi: 10.1517/14712598.8.6.713.
- Jiajun Gu and Jun S. Liu. Bayesian biclustering of gene expression data. *BMC Genomics*, 9(Suppl 1):S4, March 2008. ISSN 1471-2164. doi: 10.1186/1471-2164-9-S1-S4. PMID: 18366617.
- J. A. Hartigan. Direct clustering of a data matrix. *Journal of The American Statistical Association - J AMER STATIST ASSN*, 67(337):123–129, 1972. doi: 10.1080/01621459.1972.10481214.
- Trevor Hastie, Robert Tibshirani, Gavin Sherlock, Michael Eisen, Patrick Brown, and David Botstein. Imputing missing data for gene expression arrays. Technical report, 1999.
- Sepp Hochreiter, Ulrich Bodenhofer, Martin Heusel, Andreas Mayr, Andreas Mitterecker, Adetayo Kasim, Tatsiana Khamiakova, Suzy Van Sanden, Dan Lin, Willem Talloen, Luc Bijmens, Hinrich W. H. Ghlmann, Ziv Shkedy, and Djork-Arn Clevert. FABIA: factor analysis for bicluster acquisition. *Bioinformatics*, 26(12):1520–1527, June 2010. ISSN 1367-4803, 1460-2059. doi: 10.1093/bioinformatics/btq227. PMID: 20418340.
- Jui-Hung Hung, Troy W. Whitfield, Tun-Hsiang Yang, Zhenjun Hu, Zhiping Weng, and Charles DeLisi. Identification of functional modules that correlate with phenotypic difference: the influence of network topology. *Genome Biology*, 11(2):R23, February 2010. ISSN 1465-6906.
- Curtis Huttenhower, K. Tsheko Mutungu, Natasha Indik, Woongcheol Yang, Mark Schroeder, Joshua J. Forman, Olga G. Troyanskaya, and Hilary A. Collier. Detailing regulatory networks through large scale data integration. *Bioinformatics*, 25(24):3267–3274, December 2009. ISSN 1367-4803, 1460-2059. doi: 10.1093/bioinformatics/btp588. PMID: 19825796.
- Daxin Jiang, Chun Tang, and Aidong Zhang. Cluster analysis for gene expression data: a survey. *IEEE Transactions on Knowledge and Data Engineering*, 16(11):1370–1386, November 2004. ISSN 1041-4347. doi: 10.1109/TKDE.2004.68.
- Sebastian Kaiser, Rodrigo Santamaria, Roberto Theron, Luis Quintales, and Friedrich Leisch. biclust: Bicluster algorithms. *R package version 1.0.2*, 2, 2009.
- Guy Karlebach and Ron Shamir. Modelling and analysis of gene regulatory networks. *Nature Reviews Molecular Cell Biology*, 9(10):770–780, October 2008. ISSN 1471-0072. doi: 10.1038/nrm2503.

- Yuval Kluger, Ronen Basri, Joseph T. Chang, and Mark Gerstein. Spectral biclustering of microarray data: Coclustering genes and conditions. *Genome Research*, 13(4):703–716, April 2003. ISSN 1088-9051, 1549-5469. doi: 10.1101/gr.648603. PMID: 12671006.
- Hans-Peter Kriegel, Peer Krger, and Arthur Zimek. Clustering high-dimensional data: A survey on subspace clustering, pattern-based clustering, and correlation clustering. *ACM Trans. Knowl. Discov. Data*, 3(1):1:11:58, March 2009. ISSN 1556-4681. doi: 10.1145/1497577.1497578.
- Sheryl R. Krig, Seth Frietze, Catalina Simion, Jamie K. Miller, Will H. D. Fry, Hanine Rafidi, Lakmal Kotelawala, Lihong Qi, Obi L. Griffith, Joe W. Gray, Kermit L. Carraway, and Colleen Sweeney. Lrig1 is an estrogen-regulated growth suppressor and correlates with longer relapse-free survival in ER-positive breast cancer. *Molecular Cancer Research*, 9(10):1406–1417, October 2011. ISSN 1541-7786, 1557-3125. doi: 10.1158/1541-7786.MCR-11-0227.
- Laura Lazzeroni and Art Owen. Plaid models for gene expression data. *Statistica Sinica*, 12:6186, 2000.
- Jeffrey Leek and John Storey. Capturing heterogeneity in gene expression studies by surrogate variable analysis. *PLoS Genet*, 3(9):e161–1735, 2007. ISSN 1553-7404. doi: 10.1371/journal.pgen.0030161.
- Jeffrey T. Leek, Robert B. Scharpf, Hector Corrada Bravo, David Simcha, Benjamin Langmead, W. Evan Johnson, Donald Geman, Keith Baggerly, and Rafael A. Irizarry. Tackling the widespread and critical impact of batch effects in high-throughput data. *Nature Reviews Genetics*, 11(10):733–739, October 2010. ISSN 1471-0056. doi: 10.1038/nrg2825.
- Guojun Li, Qin Ma, Haibao Tang, Andrew H. Paterson, and Ying Xu. QUBIC: a qualitative biclustering algorithm for analyses of gene expression data. *Nucleic Acids Research*, 37(15):e101–e101, August 2009. ISSN 0305-1048, 1362-4962. doi: 10.1093/nar/gkp491. PMID: 19509312.
- Jennifer Listgarten, Carl Kadie, Eric Schadt, and David Heckerman. Correction for hidden confounders in the genetic analysis of gene expression. *Proceedings of the National Academy of Sciences of the United States of America*, 107(38):16465–16470, 2010. ISSN 1091-6490. doi: 10.1073/pnas.1002425107.
- Lesley T. MacNeil and Albertha J. M. Walhout. Gene regulatory networks and the role of robustness and stochasticity in the control of gene expression. *Genome Research*, 21(5):645–657, May 2011. ISSN 1088-9051, 1549-5469. doi: 10.1101/gr.097378.109.
- Sara C. Madeira and Arlindo L. Oliveira. Biclustering algorithms for biological data analysis: A survey. *IEEE/ACM Trans. Comput. Biol. Bioinformatics*, 1(1):2445, January 2004. ISSN 1545-5963. doi: 10.1109/TCBB.2004.2.
- Sara C Madeira and Arlindo L Oliveira. A polynomial time biclustering algorithm for finding approximate expression patterns in gene expression time series. *Algorithms for*

- molecular biology: AMB*, 4:8, 2009. ISSN 1748-7188. doi: 10.1186/1748-7188-4-8. PMID: 19497096 PMCID: PMC2709627.
- Julien Mairal, Francis Bach, Jean Ponce, and Guillermo Sapiro. Online learning for matrix factorization and sparse coding. *J. Mach. Learn. Res.*, 11:19–60, 2010. ISSN 1532-4435.
- T M Murali and Simon Kasif. Extracting conserved gene expression motifs from gene expression data. *Pacific Symposium on Biocomputing. Pacific Symposium on Biocomputing*, pages 77–88, 2003. ISSN 2335-6936. PMID: 12603019.
- Nikita Boyko Neng Fan. Recent advances of data biclustering with application in computational neuroscience. pages 105–132, 2009. doi: 10.1007/978-0-387-88630-5_6.
- Juuso A. Parkkinen and Samuel Kaski. Searching for functional gene modules with interaction component models. *BMC Systems Biology*, 4(1):1–11, December 2010. ISSN 1752-0509.
- A. Patrikainen and M. Meila. Comparing subspace clusterings. *IEEE Transactions on Knowledge and Data Engineering*, 18(7):902–916, July 2006. ISSN 1041-4347. doi: 10.1109/TKDE.2006.106.
- Joseph K. Pickrell, John C. Marioni, Athma A. Pai, Jacob F. Degner, Barbara E. Engelhardt, Everlyne Nkadori, Jean-Baptiste Veyrieras, Matthew Stephens, Yoav Gilad, and Jonathan K. Pritchard. Understanding mechanisms underlying human gene expression variation with RNA sequencing. *Nature*, 464(7289):768–772, April 2010. ISSN 0028-0836. doi: 10.1038/nature08872.
- Amela Preli, Stefan Bleuler, Philip Zimmermann, Anja Wille, Peter Buhlmann, Wilhelm Gruissem, Lars Hennig, Lothar Thiele, and Eckart Zitzler. A systematic comparison and evaluation of biclustering methods for gene expression data. *Bioinformatics*, 22(9):1122–1129, May 2006. ISSN 1367-4803, 1460-2059. doi: 10.1093/bioinformatics/btl060. PMID: 16500941.
- Robert G. Ramsay and Thomas J. Gonda. MYB function in normal and cancer cells. *Nature Reviews Cancer*, 8(7):523–534, July 2008. ISSN 1474-175X. doi: 10.1038/nrc2439.
- Michael Reich, Ted Liefeld, Joshua Gould, Jim Lerner, Pablo Tamayo, and Jill P. Mesirov. GenePattern 2.0. *Nature Genetics*, 38(5):500–501, May 2006. ISSN 1061-4036. doi: 10.1038/ng0506-500.
- Jianhua Ruan, Angela K. Dean, and Weixiong Zhang. A general co-expression network-based approach to gene expression analysis: comparison and applications. *BMC Systems Biology*, 4(1):8, February 2010. ISSN 1752-0509. doi: 10.1186/1752-0509-4-8.
- Rodrigo Santamara, Luis Quintales, and Roberto Thern. Methods to bicluster validation and comparison in microarray data. In Hujun Yin, Peter Tino, Emilio Corchado, Will Byrne, and Xin Yao, editors, *Intelligent Data Engineering and Automated Learning - IDEAL 2007*, number 4881 in Lecture Notes in Computer Science, pages 780–789. Springer Berlin Heidelberg, January 2007. ISBN 978-3-540-77225-5, 978-3-540-77226-2.

- Juliane Schafer and Korbinian Strimmer. An empirical bayes approach to inferring large-scale gene association networks. *Bioinformatics*, 21(6):754–764, March 2005a. ISSN 1367-4803, 1460-2059. doi: 10.1093/bioinformatics/bti062.
- Juliane Schafer and Korbinian Strimmer. A shrinkage approach to large-scale covariance matrix estimation and implications for functional genomics. *Statistical Applications in Genetics and Molecular Biology*, 4(1), November 2005b.
- Markus Schroeder, Benjamin Haibe-Kains, Aedin Culhane, Christos Sotiriou, Gianluca Bontempi, and John Quackenbush. *breastCancerNKI: Geneexpression dataset published by Van't Veer et al. [2002] and van de Vijver et al. [2002] (NKI).*, 2011. R package version 1.0.6.
- Marcilio CP de Souto, Ivan G. Costa, Daniel SA de Araujo, Teresa B. Ludermitz, and Alexander Schliep. Clustering cancer gene expression data: a comparative study. *BMC Bioinformatics*, 9(1):497, November 2008. ISSN 1471-2105. doi: 10.1186/1471-2105-9-497.
- Oliver Stegle, Leopold Parts, Richard Durbin, and John Winn. A bayesian framework to account for complex non-genetic factors in gene expression levels greatly increases power in eqtl studies. *PLoS computational biology*, 6(5):e1000770, 2010. ISSN 1553-7358. doi: 10.1371/journal.pcbi.1000770.
- Vasiliki Theodorou, Rory Stark, Suraj Menon, and Jason S. Carroll. GATA3 acts upstream of FOXA1 in mediating ESR1 binding by shaping enhancer accessibility. *Genome Research*, 23(1):12–22, January 2013. ISSN 1549-5469. doi: 10.1101/gr.139469.112.
- Heather Turner, Trevor Bailey, and Wojtek Krzanowski. Improved biclustering of microarray data demonstrated through systematic performance tests. *Computational Statistics & Data Analysis*, 48(2):235–254, February 2005. ISSN 0167-9473. doi: 10.1016/j.csda.2004.02.003.
- Marc J. Van de Vijver, Yudong D. He, Laura J. Van Veer, Hongyue Dai, Augustinus A. M. Hart, Dorien W. Voskuil, George J. Schreiber, Johannes L. Peterse, Chris Roberts, Matthew J. Marton, Mark Parrish, Douwe Atsma, Anke Witteveen, Annuska Glas, Leonie Delahaye, Tony van der Velde, Harry Bartelink, Sjoerd Rodenhuis, Emiel T. Rutgers, Stephen H. Friend, and Ren Bernards. A gene-expression signature as a predictor of survival in breast cancer. *The New England Journal of Medicine*, 347(25):1999–2009, December 2002. ISSN 1533-4406. doi: 10.1056/NEJMoa021967.
- Iven Van Mechelen, Hans-Hermann Bock, and Paul De Boeck. Two-mode clustering methods: a structured overview. *Statistical methods in medical research*, 13(5):363–394, October 2004. ISSN 0962-2802. PMID: 15516031.
- Laura J. van 't Veer, Hongyue Dai, Marc J. van de Vijver, Yudong D. He, Augustinus A. M. Hart, Mao Mao, Hans L. Peterse, Karin van der Kooy, Matthew J. Marton, Anke T. Witteveen, George J. Schreiber, Ron M. Kerkhoven, Chris Roberts, Peter S. Linsley, Ren Bernards, and Stephen H. Friend. Gene expression profiling predicts clinical outcome of breast cancer. *Nature*, 415(6871):530–536, January 2002. ISSN 0028-0836. doi: 10.1038/415530a.

- Laura J. Vant Veer, Hongyue Dai, Marc J. van de Vijver, Yudong D. He, Augustinus A. M. Hart, Mao Mao, Hans L. Peterse, Karin van der Kooy, Matthew J. Marton, Anke T. Witteveen, George J. Schreiber, Ron M. Kerkhoven, Chris Roberts, Peter S. Linsley, Rene Bernards, and Stephen H. Friend. Gene expression profiling predicts clinical outcome of breast cancer. *Nature*, 415(6871):530–536, January 2002. ISSN 0028-0836. doi: 10.1038/415530a.
- Y. Wang, E. J. Poulin, and R. J. Coffey. LRIG1 is a triple threat: ERBB negative regulator, intestinal stem cell marker and tumour suppressor. *British Journal of Cancer*, 108(9):1765–1770, March 2013. ISSN 0007-0920. doi: 10.1038/bjc.2013.138.
- M. West. Bayesian factor regression models in the "large p, small n" paradigm. *Bayesian Statistics 7*, pages 723–732, 2003.
- Daniela M. Witten, Robert Tibshirani, and Trevor Hastie. A penalized matrix decomposition, with applications to sparse principal components and canonical correlation analysis. *Biostatistics*, 10(3):515–534, jul 2009. ISSN 1468-4357. doi: 10.1093/biostatistics/kxp008.
- Zhengming Xing, Mingyuan Zhou, Alexey Castrodad, Guillermo Sapiro, and Lawrence Carin. Dictionary learning for noisy and incomplete hyperspectral images. *SIAM J. Img. Sci.*, 5(1):33–56, January 2012. ISSN 1936-4954. doi: 10.1137/110837486.
- Sungroh Yoon, Luca Benini, and Giovanni De Micheli. Co-clustering: a versatile tool for data analysis in biomedical informatics. *IEEE transactions on information technology in biomedicine: a publication of the IEEE Engineering in Medicine and Biology Society*, 11(4):493–494, July 2007. ISSN 1089-7771. PMID: 17674632.
- Bin Zhang and Steve Horvath. A general framework for weighted gene co-expression network analysis. *Statistical Applications in Genetics and Molecular Biology*, 4(1), August 2005.
- Mei Hong Zhang, Hong Tao Man, Xiao Dan Zhao, Ni Dong, and Shi Liang Ma. Estrogen receptor-positive breast cancer molecular signatures and therapeutic potentials (review). *Biomedical Reports*, 2(1):41–52, January 2014. ISSN 2049-9434. doi: 10.3892/br.2013.187.
- Mingyuan Zhou, Haojun Chen, Lu Ren, Guillermo Sapiro, Lawrence Carin, and John W. Paisley. Non-parametric bayesian dictionary learning for sparse image representations. In Y. Bengio, D. Schuurmans, J.D. Lafferty, C.K.I. Williams, and A. Culotta, editors, *Advances in Neural Information Processing Systems 22*, pages 2295–2303. Curran Associates, Inc., 2009.